



List of contents

Preface.....	2
Summary	3
1. Introduction.....	5
1.1. Objectives.....	14
2. Material and methods.....	15
2.1. Experimental design.....	15
<i>Earthworm culture</i>	15
<i>Acclimation and exposure conditions</i>	16
<i>Irradiation</i>	16
<i>Dosimetry</i>	17
<i>Earthworm fixation</i>	17
2.2. Analysis of the apoptotic activity	18
2.3. Statistical treatments	20
3. Results	20
3.1. Comparison of methods.....	31
4. Discussion.....	32
4.1. Inter-comparison between the methods.....	32
4.2. Tissue apoptotic response.....	33
4.3. Ecosystem relevance	35
4.4. Effect of Temperature	38
4.5. Conclusions and future work.....	39
5. References.....	40

Preface

This study is a part of EANOR project (Long-term consequences of enhanced radioactivity and conventional chemical pollutants for biota at the scale of individuals, population and communities) and was performed in cooperation with the university of Lyon, France.

I would like to thank my supervisors, Prof. Dr Deborah Oughton, Prof. Dr Brit Salbu, Head of the Isotope Laboratory, and Dr Turid Hertel-Aas, for giving me opportunity to be involved in this very interesting project, for their precious guiding and their great kindness and disponibility.

I would like to thank also Prof. Jean-Marie Exbrayat for his great help and for kindly letting me use the equipments of his laboratory, at the university of Lyon. A great thank also to Elara Moudilou, from the same team, for her numerous advices and her technical assistance.

I want to thank also Dr Ole Christian Lind for his help and for letting use the Gamma Radiation Facility (GRF) at NMBU/CERAD CoE.

A special thank to NFR and EANET for financial support.

And finally, I'd like to thank my family and friends for their presence and their permanent support.

NMBU, Ås, 11.12.2014

Emmanuel Lapied

Summary

Earthworms are organisms of key importance worldwide. As ecosystem engineers, they constitute one of the main structuring agents of most soil ecosystems. Previous studies have concluded that earthworms appear to be among the most radiosensitive component of the soil fauna, and decreases in populations have been observed following accidents. Radiosensitivity varies with the developmental stage, with immatures being more radiosensitive than adults. However, little is known about the mechanisms of radiation impact on earthworms. At the ultrastructural scale and as organisms living in close contact with soil, earthworms developed efficient immune and apoptotic systems. This mainly caspase- and mitochondria-dependent system controls and regulates cell proliferation and elimination of damaged cells. Since apoptosis is known to be a central mechanism in the biological response to irradiation, better understanding of this cell process after radiation exposure is of first interest.

The aim of this work is to shed a new light on potential impacts of low total doses of ionizing gamma radiations on the apoptotic activity in earthworms and on their physiological capacity to withstand a certain level of irradiation. The study design was based on irradiation of the earthworm species *Eisenia fetida* during 7 days at 0, 0.14 and 10 mGy.h⁻¹, this level of exposure being known to reduce the cocoon hatchability, and at 10°C and 20°C to investigate any impact of temperature. Three different apoptosis methods (TUNEL, Apostain and caspase 3 staining) were tested on five different tissues: cuticule, circular and longitudinal musculatures, intestinal epithelium and chloragogenous matrix.

Our results confirmed the applicability of apoptosis as a useful and reliable biomarker for radiation impacts on earthworms. The three different staining methods gave comparable results although some statistically significant differences seem to indicate that caspase 3 labeling could have a better detection limit. Three major results were obtained: 1) within a given tissue, an exposure to 10 mGy.h⁻¹ of external γ -radiation always led to an increase of the number of apoptotic cells comparing to the controls; 2) in all groups, the intestinal epithelium and chloragogenous matrix showed a higher level of apoptosis (up to six times higher) compared to the other tissue types; and 3) the temperature (10°C and 20°C) had probably low or no effects on the apoptotic signal.

The result tends to show that, after only 7 days of exposure at a dose-rate known to reduce the cocoon hatchability (albeit at longer times and higher total doses), ionizing radiations trigger an apoptotic response in tissues constituting the major part of the animal body. This means that the biomarker may be a useful early indicator of potential negative effects, given that the dose rates are known to result in negative impacts at the organism level. In addition, such a level of programmed cell death in the intestinal and chloragogenous cells may have heavy consequences for the earthworms. The intestinal epithelium plays a central role in the absorption of nutrients, while the chloragogenous tissue, covering the external pared of the intestine, is a crucial organ in the ionic balance and the immune system. Potential damages or over-stimulation of the apoptosis after irradiation might dramatically affect crucial physiological processes controlled by these structures. Moreover, their localization at the interface between interior and exterior medium may explain their high reactivity comparing to the other tissues.

In spite of comparable results between the three tested methods, differences are notable. Thus, a lower apoptotic activity was revealed by caspase 3 labeling, for almost all treatments, with only high levels being seen in the longitudinal musculature at 10°C and 10 mGy.h⁻¹. In addition, the caspase 3 labeling method was the only one that showed a statistically significant increase at only 0.14 mGy.h⁻¹. The more sensitive detection limit could reflect the relatively low level of background apoptosis in controls compared to the other treatments. Hence a combination of at least caspase 3 labelling and TUNEL or Apostain would be recommended for studies on this mechanism in earthworms.

This study constitutes one of the very first report and description of the apoptotic process in earthworms and, after antibody labeling, represents a pioneer work in showing the conservation of caspase 3 proteins in earthworms. This latest result is of high interest considering the central role of caspase 3 in the control of the apoptotic cascade in particular as a molecule regulated by mitochondria through the release of cytochrome c. In addition, the results obtained in this work could be relevant in our understanding of potential links between apoptosis and radiosensitivity.

1. Introduction

Earthworms are organisms of major importance in soils worldwide, both in terms of biomass and activity, and have a heavy impact on the soil functioning. As ecosystem engineers, they constitute one of the main structuring agents of the soil ecosystem and a crucial link between the belowground and the aboveground biocenosis (Jones et al. 1994). In Europe, for instance, earthworm biomass is commonly in a range of 400 to 700 kg fresh weight.ha⁻¹ and reached 500 to 2000 kg or more in grasslands (Edwards & Bohlen 1996). In this very populated region, earthworm biomass is on average higher than biomass of humans. Such abundance deeply influences the complex interactions between the three main living fractions of soils driving the organic matter decomposition and recycling processes (Lee 1985; Lavelle & Spain 2001).

Indeed, the microfauna is composed by microscopic animals (<0.2 mm), including nematodes, small arthropods and protozoans. This fauna, together with the soil bacteria and fungi, is very active as organic matter decomposers. The mesofauna, between 0.2 and 1 mm, includes mainly nematodes, acarians, rotifers and collembolas (Hopkin 1997). This animal guild fractionates large particles of organic matter and greatly facilitates the decomposition activity of the microorganisms. The macrofauna, the most visible fringe of the soil fauna, is mainly composed and largely dominated by earthworms, ants and large arthropod larvae (Lavelle & Spain 2001). This animal fraction is the motor of the soil bioturbation, contributing to the air and organic matter circulation within the soil layers and the fragmentation of the soil litter. The burrow network built by earthworms within their zone of activity, or drilosphere, helps the penetration of root systems in depth and favors the soil drainage by increasing the soil macroporosity (figure 1). In addition, the soil transit through the earthworm digestive tract and the production of large volumes of casts play a role of incubator for various functional groups of microorganisms, including numerous species specialized in the organic matter decomposition.

Earthworms constitute a very diversified group and are largely distributed worldwide in almost all types of ecosystems and climates, except in the deserts and the polar areas (Edwards & Bohlen 1996; Lapied 2014). Associated to an often dominant biomass, their low capacity of movement favors a high regional species diversity, usually higher than most of the rest of the

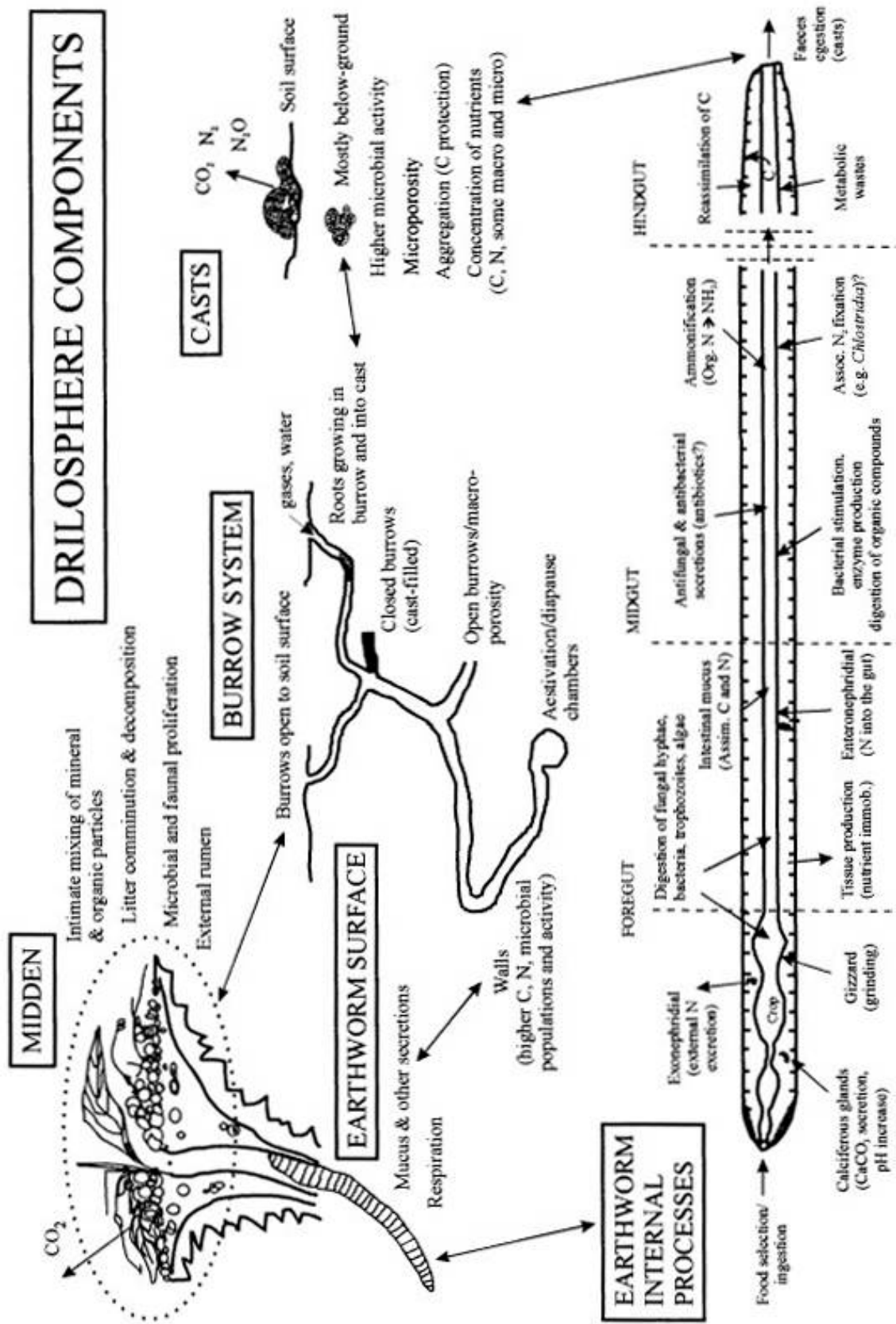


Figure 1: Components of the drilosphere and some associated properties and processes. From Brown 1995.

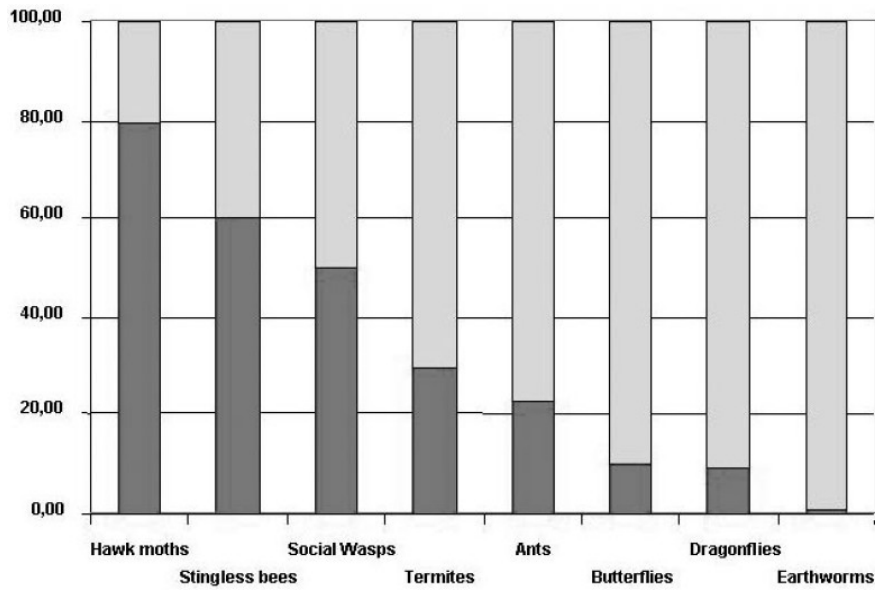


Figure 2: Estimated ratios of local to regional diversity in different groups of invertebrates in the Guayana Shield region. From Lavelle and Lapied 2003.

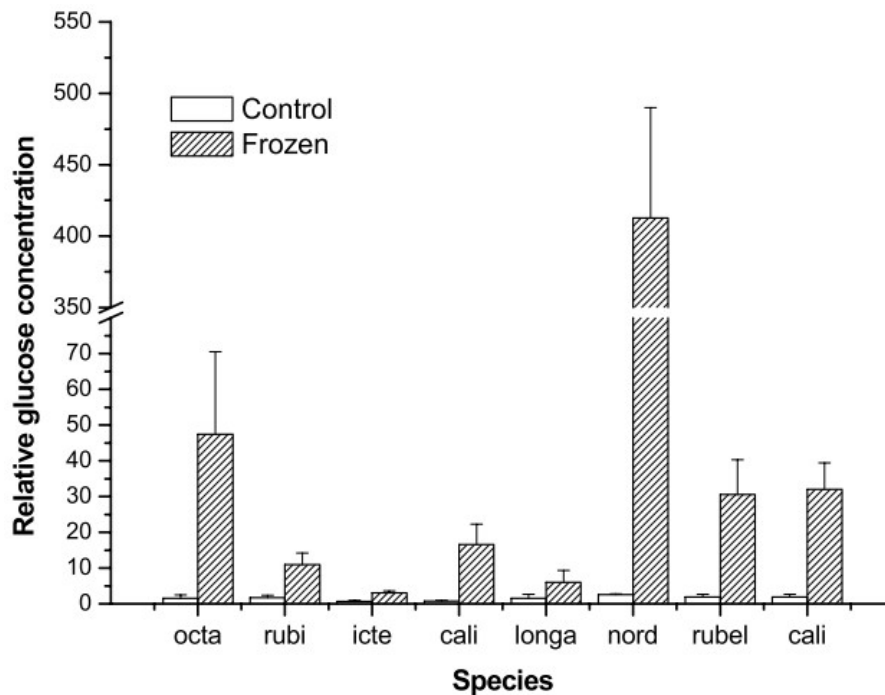


Figure 3: Glucose accumulation (relative units) in freeze-tolerant and freeze-intolerant earthworm species after being frozen at -1.5°C for 24 hours. Freeze-tolerant species: *Dendrobaena octaedra* (octa), *Eisenia nordenskioldi* (nord). Freeze-intolerant species: *Dendrodrilus rubidus* (rubi), *Aporrectodea icterica* (icte), *Aporrectodea caliginosa* (cali) (data from two different studies), *Allolobophora longa* (longa), *Lumbricus rubellus* (rubel). From Holmstrup 2003.

invertebrate fauna (figure 2). Temperatures and rainfalls are the main environmental factors determining the life-cycle and community composition of earthworms (Lavelle 1983). Low temperatures, such as 10°C or below for species living in temperate areas, slow down the maturation process, the production of cocoons and often lead to a specific metabolic dormancy: the diaposis, an equivalent of the hibernation observed in mammals (Edwards & Bohlen 1996; Fayolle et al. 1997). Still lower temperatures, approaching the freezing point, drive to specific physiological adaptations in few well adapted species, including an accumulation of glucose in the body (figure 3) (Holmstrup 2003). *Eisenia fetida*, for instance, the main research model of earthworm worldwide and originating from temperate Europe, has an optimal temperature around 18-20°C.

Recently, earthworms emerged as particularly sensitive organisms to soil disturbances and toxic contaminations (Morgan 1998, 1999; Nahmani 2003; Lapied 2009). However to date, despite an increasing number of scientific investigations, rather little is known about the impact of ionizing radiations on soil organisms, including the soil macrofauna. Globally, the radiosensitivity of soil invertebrates is highly variable, from 20 to 5000 Gy (LD50) and is strongly dependent on the developmental stage (Fesenko 2005). For Sarapultsev & Geras'kin (1993), ontogenesis radiosensitivity of invertebrates can vary of more than two orders of magnitude. Disorders in the reproduction process were observed at doses corresponding to 10 % of LD50 (Krivolutsky 1994). According to Krivolutsky et al. (Krivolutsky et al. 1990; Krivolutsky 1994), a clear reduction in the invertebrates density was visible in the forest litter of the Chernobyl area at total doses of around 8 Gy. In earthworms, adults seem to be among the most radioresistant multicellular animals (Geras'kin 2008), but not the juvenile stages which are considered to have a LD50 comparable to mice (Krivolutsky 1983). Previous studies at room temperature (20-22°C) have shown no negative effects on the reproductive capacity of the earthworm species *E. fetida* exposed for 12 weeks at 0.135 mGy.h⁻¹ (Hertel-Aas et al. 2011) or during exposure of two subsequent generations at 0.17-0.19 mGy.h⁻¹ (Hertel-Aas et al. 2007), whereas exposure at 11 mGy.h⁻¹ resulted in a pronounced reduction of cocoon hatchability after 5 to 8 weeks (Hertel-Aas et al. 2007, 2011).

At the ultrastructural scale and as animal organisms living in soils, an environment particularly rich in microorganisms including potential bacterial and viral pathogens, earthworms

developed an efficient immune system, to track down and remove external aggressors, and a powerful apoptotic system, a major tool to control and eliminate deficient cells (figure 4). Thus, earthworm tissues are permanently subject to apoptosis. This cell process, a form of programmed cell death mainly caspase- and mitochondria-dependent, is one of the most ancient and universal cell processes within living organisms in the control and regulation of cell proliferation and in the elimination of damaged cells (Ameisen 1996; Aravind 1999). Today, the apoptotic cascade occurs in all multicellular organisms including all plant and animal forms (Saran 2000; Samuilov 2000; Estabel et al. 2003). Even unicellular microorganisms are believed to perform such a form of cell process (Lewis 2000; Ning 2002).

Apoptosis analysis has become widespread in toxicology (Roberts 2000). In terms of ecotoxicological tests, the apoptotic response to a stress linked to a toxic contamination appears to be more sensitive compared to classical physiological tests, such as mortality, reproduction or growth tests. This type of analysis, helped by the recent progresses in immunohistochemistry, open a new window for the fine understanding of the cell and molecular mechanisms underlying a toxicological response. It has also been used in studies of the potential radiosensitivity of humans (Zellweger et al. 2003; Ou et al. 2012). However, to date, few studies have focused on apoptosis in earthworms (Espinoza-Navarro 2005) although it has been recognized as a good biomarker of a metallic stress (Santos Amaral 2005).

Among the immunohistochemical methods to detect apoptosis, TUNEL, Apostain and caspase 3 staining are widely used today. Described at the beginning of the 1990s, TUNEL became quickly a major method for detecting apoptotic programmed cell death (Garvrieli et al. 1992). This staining method is based on the presence of specific nicks in terminal position of DNA fragments formed during the apoptotic process. These nicks are localized by a terminal deoxynucleotidyl transferase (TdT), an enzyme that will catalyze the addition of deoxyuridine-triphosphatase (dUTPs), secondarily labeled with an appropriate marker. Its action mode allows this method to identify cells in the last phase of apoptosis (Negoescu et al. 1996, 1998).

The Apostain staining method uses the monoclonal antibody F7-26 to detect apoptotic single-stranded DNA (ssDNA) after double-stranded DNA opening. This technique, elaborated at the end of the 1990s (Ferlini et al. 1997; Frankfurt & Krishan 2001), relies on the transient changes

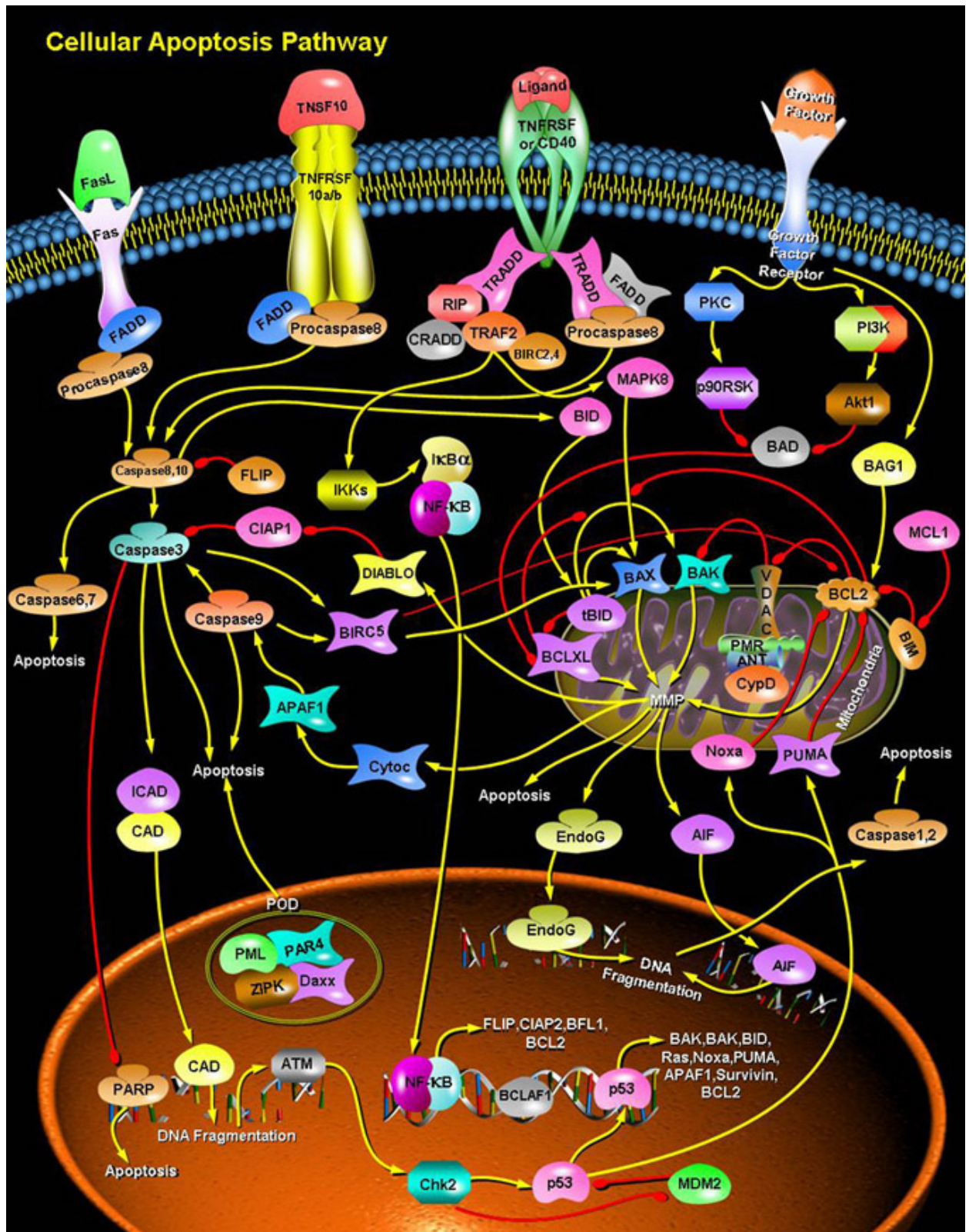


Figure 4: Overview of the cellular apoptosis pathways. From Biologend, 2008.

of chromatin texture occurring in early apoptosis. At this step, cells engaged in a programmed death process have still an integer plasma membrane.

The method based on the caspase 3 intra-cell detection relies on the use of an anti-active Caspase 3 primary antibody which preferentially recognizes the p17 fragment of the active Caspase 3 (Salvesen 2002). Caspases belong to a family of cysteine-aspartic acid protease and are members of the interleukin-1 β -converting enzyme family (Alnemri et al., 1996; Chowdhury et al., 2008). These molecules are responsible for chromatin condensation and DNA fragmentation (Porter and Jänicke, 1999). Thus, their sequential activation plays a central role in the execution-phase of cell apoptosis (figure 4). In mammals, caspase-3 is activated in the apoptotic cell both by extrinsic (death ligand) and intrinsic (mitochondrial) pathways (Salvesen, 2002; Ghavami et al., 2009). Briefly, after activation by an executioner caspase, the caspase-3 zymogen (extrinsic pathway), caspase 3 cleaves numerous proteins, including nuclear lamins, key fibrous proteins providing structural function and transcriptional regulation in the cell nucleus. In intrinsic activation, cytochrome c is released from the mitochondria to constitute a growing signal cascade. In a simplified way, this cytochrome c will work in combination with caspase-9, apoptosis-activating factor 1 (Apaf-1) and ATP to create the apoptosome and process procaspase-3 (Katunuma et al., 2001; Li et al., 2004). Activated by this latest, caspase 3 will then cleave the actin cytoskeleton. In an evolution point of view, aspartate-specific cysteine proteases are highly conserved molecules and recent progresses have been made in the knowledge of non-mammalian caspases, such as caspase-like-proteases, paracaspases and metacaspases (Chowdhury et al. 2008). Whether they constitute orthologous genes in invertebrates still remains unknown.

In animals, it is admitted that most cell types and tissues have the capacity to trigger a process of programmed cell death (Ameisen 1996; Estabel et al. 2003). In earthworms, except within the first tens of segments where reproductive organs and differentiated elements of the digestive tract are localized, the largest part of the body is occupied by the intestinal region and five main tissue types: the cuticule, the longitudinal and circular musculatures, the intestinal epithelium and the chloragogenous matrix (figures 5 and 6). The cuticule constitutes the first barrier, both mechanical and immune, against external mechanical, chemical or biological potential aggressions. It is an external integument of epidermal origin and composed of layers

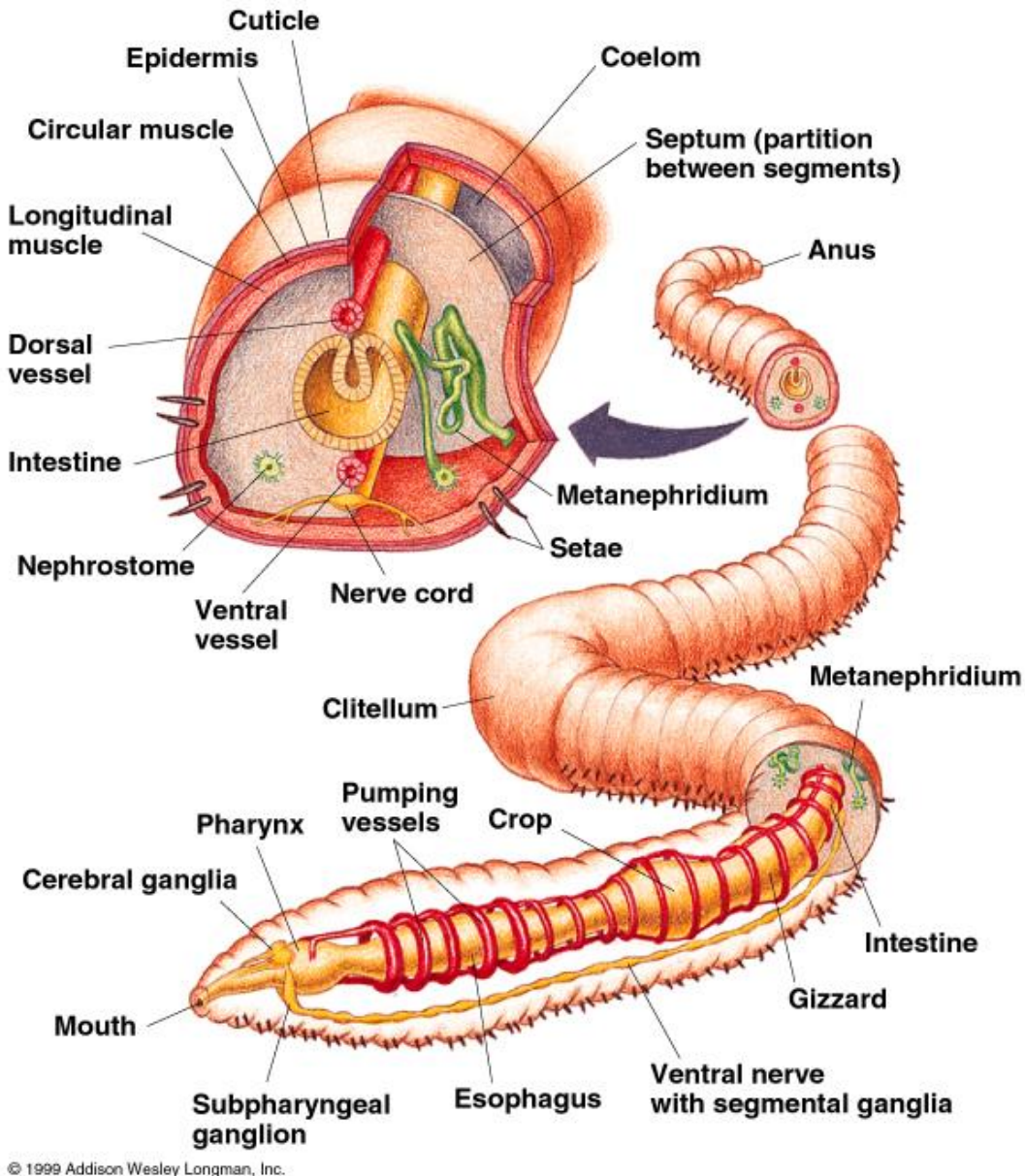


Figure 5: Overview of the earthworm internal morphology of earthworms. From Addison Wesley Longman, Inc. 1999.

of parallel collagen fibres (Richards 1977). Although permeable to respiratory gases and being perforated at the numerous epidermal secretory cell openings, it offers significant resistance to abrasion. Large granular, epidermal orthochromatic cells secrete, through the cuticle, an abundant mucus mainly composed in a mucopolysaccharide-protein-lipid complex and functioning as viscoelastic lubricant during locomotion (Jamieson 1981). In addition, the mucus takes part in the humoral immune system in earthworms through the production of numerous

polymorphic and multifunctional proteins, including cytolytic and antibacterial, such as fetidins (Roch 1981; Milochau 1997). Mixed with mucous, fetidins cover the entire body constituting an external non-specific anti-microbial barrier (Valembois 1985).

The earthworm intestine has the potential for high exposure from contaminated soil. After transit through the first part of the gut, ingested soil or water enter the intestine for a long period (intestine occupies, in *Eisenia fetida*, 80 % to 90 % of the total body length). Intestine is divided into 3 ultrastructurally and physiologically different parts: the anterior intestine, the mid-intestine and the posterior intestine (Jamieson 1981). The first 5 segments constitute the anterior intestine, characterised by specific wide folds in the internal wall, the beginning of the typhlosole (a dorsal invagination of the wall which increase the intestinal absorption surface). The epithelium is rich in non-specific esterases, acid and alkaline phosphatases. The approximately 20 following segments constitute the mid-intestine. The typhlosole here shows maximal development forming a thick longitudinal dorsal ribbon, and the dorsal region, including the typhlosole, consists of glandular and ciliated cells whereas the ventral wall has only ciliated cells (Jamieson 1981). This region also secretes mucus, a readily assimilable C source. After a 10-15 segments transition, the following 50-110 segments constitute the posterior intestine, rich in alkaline phosphatase but where the esterase activity is less important. This region secretes the mucous peritrophic membrane which is believed to play a role in digestion and ultrafiltration (Jamieson 1981). Numerous enzymes are secreted within the intestine. The internal environment thus created, associated with an intense secretion of mucus, CaCO₃ (produced upstream in the oesophagous region by calciferous glands), peroxydases, antibiotics and bacteriostatics, plays a major role in the ingested soil transit, absorption and microbiota establishment (Brown 1995).

The chloragogenous tissue is considered in annelids to resemble the vertebrate liver function, in particular in the metabolism and storage of glycogen, storing lipids and excretion (Roots 1960; Richards & Ireland 1978; Jamieson 1981). Briefly, the chloragogenous tissue covers the external wall of the intestine on its entire length. This highly irrigated cell matrix is constituted in modified peritoneal cells, the chloragocytes. Chloragogenous tissue also taking a great part in the ionic regulation, including acid-base and electron balance (Fischer & Trombitas 1980), is able to bind xenobiotics (such as pesticides) and to sequester metals (Ireland & Fisher 1978;

Richards & Ireland, 1978; Morgan et al. 1998, 1999). Chloragocytes, constitute a characteristic immunodefense population of earthworm leukocytes and exert, among others, a production of cytotoxic and antibacterial molecules (Valembois et al. 1982; Dales & Kalaç 1992). Their cytoplasm is filled with granules: the chloragosomes. These organelles, maybe of lysosomal origin (Varute & More 1972; Cancio et al. 1995), are positive for several enzymatic activities (acid phosphatase, β -glucuronidase, peroxidase, α -naphthyl acetate esterase) (Prentø 1986; Hønsi & Stenersen 2000) and show histochemical staining for phospholipids and acid phosphatase (Varute & More 1973; Peeters-Joris 2000). These lysosomal enzymes play a role in earthworm immune mechanisms including microbicidal action (Marks et al. 1981) as well as in wound healing (Cooper & Roch 1992).

Longitudinal and circular musculatures in earthworms constituted by smooth and striated tissues, respectively, are structures characteristic of the annelid phylum (Jamieson 1981). The longitudinal musculature is very complex. Collagens partitions transversely restrict the fibers which are connected in the longitudinal axis, thus forming a continuous syncythium along the whole animal body. Positioned perpendicularly, both tissues contract alternatively to allow a peristaltic movement of the body, origin of most horizontal and vertical movements in terrestrial annelids.

1.1. Objectives

Through a fine investigation at the cell scale of key tissues, the overall objective of the present work is to shed a new light on potential impacts of ionizing radiation on the apoptotic activity in earthworms and, by domino effect, on the physiological capacity of these organisms to withstand a certain level of gamma radiation. The hypothesis was that apoptotic effects in earthworm could be induced either earlier or at lower gamma dose-rates than reproduction effects.

The study design was based on Co-60 gamma irradiation of the earthworm species *Eisenia fetida* at relatively low overall dose rates: 0.14 and 10 mGy.h⁻¹ for 7 days. The 10 mGy.h⁻¹ dose rate was selected as a dose at which previous studies had shown negative effects on

reproduction whereas no effects were seen at longer exposure times i.e. after 5 to 8 weeks at 11 mGy.h⁻¹ (Hertel-Aas et al. 2007, 2011). In addition, irradiation was carried out at 10°C and 20°C to investigate any potential impact of temperature. As part of method development, TUNEL, Apostain and caspase 3 staining methods were chosen and applied to the cuticle, the longitudinal and circular musculatures, the intestinal epithelium and the chloragogenous matrix (figure 6). These tissues were selected both for their importance in the earthworm morphostructure and for their potential to show different response to stressors. The present results could therefore initiate further investigations to improve our understanding of the earthworm biology and to assess to which extent earthworms can be considered as relevant biological indicators in radioactive contaminated ecosystems.

2. Material and methods

The earthworm gamma exposure was carried out in December 2012 at the Gamma Radiation Facility (GRF), Norwegian University of Life Sciences, Ås, Norway.

2.1. Experimental design

Earthworm culture

The species used during this work is the earthworm model species *Eisenia fetida* (Savigny, 1826). The studied specimens came from a breeding developed on the base of individuals initially obtained from the Norwegian Center for Soil and Environmental Research (now renamed as Bioforsk Institute). Earthworms were raised in synchronous cultures in commercial potting soil at room temperature and in constant darkness for several generations. They were fed finely ground air-dried horse manure rewetted with deionized water. The substrate, composed of half soil and half manure, was changed every two months.

Artificial OECD soil was used during the acclimation and γ -irradiation phases. The soil was prepared according to OECD guideline 207 (OECD 1984) and consisted of 10 % sphagnum peat (Tiur-torv, Nittedaltorvindustri AS, Norway), 20 % kaolinite clay (China clay, 3309-25, WBB

Minerals, England UK) and 70 % industrial quartz sand (Svelviksand AS, Norway). The soil pH was measured in 0.01 M CaCl₂ and adjusted to 6.7 ± 0.1 by addition of CaCO₃. One day before use, the soil was moistened by adding deionized water to 25.8 ± 0.2 % w/w (corresponding to about 57 % of the maximum water-holding capacity). Horse manure, from the same horse (healthy and receiving no pharmaceuticals), was used as feed supply. The manure was air dried at room temperature, finely ground using a blender, sieved at 2 mm and frozen at -20°C. Just before use, the manure was thawed, and rewetted with deionized water to 67 %. The pH of the manure was 6.5 (measured in 0.01 M CaCl₂).

Acclimation and exposure conditions

Adult earthworms (28-31 weeks old) with a well-developed clitellum were used. Prior to exposure, all specimens were acclimatized in artificial OECD soil (OECD 1984) for 6 days at the same density, feeding rate and temperature (10°C or 20°C) as during the subsequent irradiation experiments. Following acclimation, the worms were washed in saline (0.85 %), weighed individually, and added to the different test boxes at random. The average wet weight of the worms was 365 ± 96 mg. A total of 100 worms were used in the experiment. The test boxes (6.1×8.1×15 cm, internal cross sectional area: 40.8 cm²) were made of black Perspex and the front side was thin (2 mm) to minimize the absorption of γ-radiation by the box material. Each replicate box contained five earthworms, 338 g moist OECD soil (50 g dry soil/specimen) and 7.5 g of moist horse manure (0.5 g dry manure/specimen/week) on the surface. The top was covered with transparent plastic.

Irradiation

E. fetida were exposed to external γ-radiation for 7 days from a ⁶⁰Co source (125 GBq) located at the Gamma Radiation Facility (GRF) at the Norwegian University of Life Sciences (NMBU)/CERAD CoE. ⁶⁰Co disintegrates by the emission of β-particles followed by emission of high energy γ-rays at two levels (1.17 and 1.33 MeV). Due to the short range of β-particles, test organisms placed in the irradiation hall were only exposed to the γ-radiation. Irradiation was carried out in a thermostatically heated room (set at either 10 or 20°C) with temperature logging every 15 min and with a cycle of 16 hours light (250–320 lx) and 8 hours dark. For

irradiation at 20°C, replicate boxes (n = 4, total 20 worms) were placed in two different distances and heights, to prevent shielding from other boxes, relative to the ^{60}Co source, resulting in absorbed dose rates of 0.14 and 10 $\text{mGy}\cdot\text{h}^{-1}$. At 10°C worms (n = 4) were only exposed at 10 $\text{mGy}\cdot\text{h}^{-1}$. Controls (n = 4) were placed in the same room, shielded by lead, and the external dose to these specimens was measured to be approximately 0.2 $\mu\text{Gy}\cdot\text{h}^{-1}$, which is within the range of natural background radiation.

Dosimetry

To be able to establish a good relationship between absorbed dose rates (doses) and observed effects, a reliable dosimetry is a prerequisite. Field dosimetry calibration was performed by the Norwegian Secondary Standard Dosimetry Laboratory (NRPA) using an ionization chamber. It was assumed that earthworm tissues had similar interaction than water and determination of the absorbed dose at the geometrical centre of the box was calculated using a correction factor for the attenuation of radiation from the front of the box to the reference point due to increased distance from the source, and from soil absorption. The specific absorption coefficient for moist OECD soil (0.0338 cm^{-1}) was calculated based on measurements using portable Mg-Ti thermoluminescence dosimeters (TLD) placed at different positions outside and inside a filled box following Hertel-Aas et al. 2007. The overall uncertainty for the dose estimation (one standard deviation) was 13%.

Earthworm fixation

Immediately after exposure, all the earthworms were sorted from the soil, washed in saline (0.85 %), dry blotted, weighed and distributed to different analysis. Totally five worms from each group, one or two from each replicate box, were fixed in a freshly made mixture (1: 9: 10) of 25 % glutaraldehyde (VWR), 0.1M PIPES (hydrogen-ion organic-based buffer, Sigma Aldrich) and 4 % paraformaldehyde (VWR) and placed at 4°C. After 24h, the worms were transferred to 0.05 M PIPES and stored at 4°C until preparation for the TUNEL, Apostain and caspase 3 assays.

2.2. Analysis of the apoptotic activity

For all experiments, earthworms were fixed in 5 % buffered formaldehyde for at least a week after harvest. Then, fixed individuals were dehydrated for 72 h, embedded in paraffin and cut into 7 µm transverse sections in the intestinal region, about 10 segments behind the clitellum. Apoptosis was examined using the TUNEL, Apostain and caspase 3 detection methods. The *in situ* Cell Death Detection Kit POD (Roche Diagnostic, Mannheim, Germany) was applied following the manufacturer's instructions to perform the TUNEL staining. Briefly, sections were successively deparaffinized, rehydrated, incubated in proteinase K (Sigma-Aldrich Chimie, Lyon, France) for 20 mn at 37°C, immersed in 3 % H₂O₂ to block endogenous peroxidases, and transferred to the reaction solution terminal deoxynucleotidyl transferase (TdT)+FITC-labelled dUTP for 60 mn at 37°C. Then, after 10 min in 1 % BSA to block non specific binding of antibodies, sections were incubated with peroxylase-conjugated anti fluorescein antibodies for 30 mn at 30°C in a humid chamber. Labelled cells could be directly detected by bright field microscopy after a DAB (3,3'-Diaminobenzidine) revelation followed by hematoxylin QS counter-staining. Negative controls were made by omitting TdT and positive controls by using DNase I at 3000 Uml⁻¹ diluted in a 50 mM Tris/HCl solution for 10 min at room temperature.

The Apostain method was performed according to the manufacture's protocol (Absys, Paris, France). This technique is based on the use of the monoclonal antibody F7-26 directed to apoptotic single-stranded DNA (ssDNA) after double-stranded DNA opening with a 56°C formamide treatment (Ferlini et al. 1997; Frankfurt & Krishan 2001). Briefly, sections were successively deparaffinized, rehydrated, incubated in a PBS (phosphate buffered saline) solution containing saponin (0.2 mg l⁻¹) and proteinase K (20 µg l⁻¹) for 20 min, incubated in 50 % formamide (V/V with distilled H₂O) for 20 mn at 58°C, immersed for 10 min in 3 % H₂O₂ to block the endogenous peroxidases and 30 mn at 37°C in 1 % BSA to block non specific binding of antibodies. Sections were then transferred to the reaction solution (monoclonal antibody F7-26) for 30 min in a humid chamber before incubation in a 1:200 dilution of secondary horse antibody (anti-mouse IgG-HRP, Immpress Vector) for 30 min. Labelled cells could be directly detected by bright field microscopy after a DAB revelation followed by hematoxylin QS counter-staining. Negative controls were performed using 1:400 diluted horse serum instead of F7-26 antibody.

The detection method of active Caspase 3 was applied following the manufacturer's instructions (Sigma-Aldrich Chimie, Lyon, France). Transverse sections of earthworm samples were permeabilized by incubation in PBS/0.1 % Triton X-100 for 5mn at room temperature, and washed three times in PBS for 5 min at room temperature. After drain, 200 μ l of blocking buffer (PBS/0.1 % Tween 20 + 5 % donkey serum) was added on each slide. Then, slides were laid flat in a humidified chamber and incubated for 2 hours at room temperature and rinsed once in PBS. 100 μ l of the active Caspase 3 antibody diluted 1/200 in blocking buffer was added and a slide with no active Caspase 3 was prepared as a negative control. Slides were then incubated in a humidified chamber overnight at 4°C before being washed three times, 10 min each in PBS/0.1 % Tween 20 at room temperature. After drain, 100 μ l of goat anti-rabbit Cy5 conjugate diluted 1:500 in PBS was added. Slides were then laid flat in a humidified chamber, protected from light, and incubated for 2 hours at room temperature before being washed three times in PBS/0.1 % Tween 20 for 5 min. Finally, slides were mounted in a permanent mounting medium.

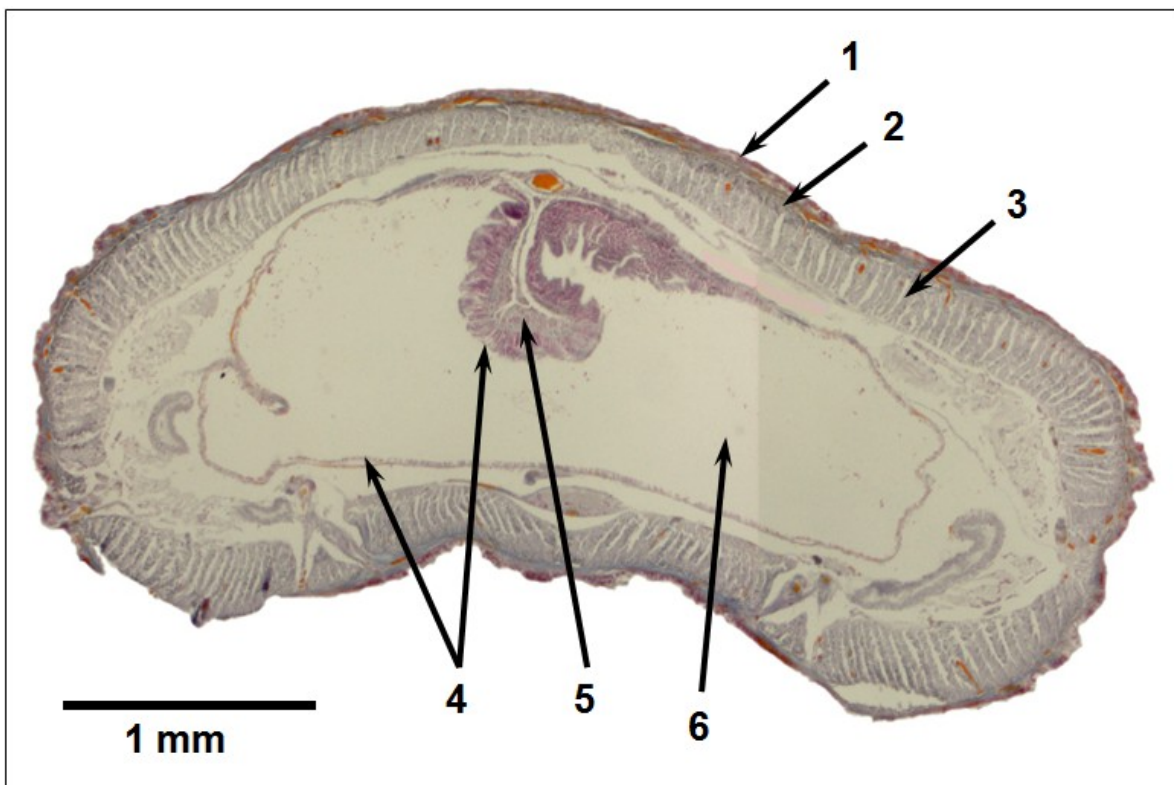


Figure 6: transversal section of the earthworm *Eisenia fetida*. 1-Cuticule. 2-Circular musculature. 3-Longitudinal musculature. 4-Intestinal epithelium. 5-Chloragogen cells. 6-Intestinal lumen.

For the three methods, stained cells were counted on histological sections in a light microscope (Nikon Eclipse E 400) connected to a Nikon DXM 1200 digital camera at 945× magnification. Counting focused on five types of tissues: cuticule, circular musculature, longitudinal musculature, intestinal epithelium and chloragogenous matrix (figure 6). In order to compare treatment effects and establish dose–response relationships, the number of TUNEL and Apostain positive stained cells per mm² was recorded. For each treatment and staining method, the number of stained cells was counted on 3 different adult earthworms, and on 5 one-mm² quadrats per tissue type per specimen (on a single histological section).

2.3. Statistical treatments

Differences between treatments regarding mean apoptotic frequency in stained cells of individual tissues were tested using the non-parametric Kruskal-Wallis test, followed by *a posteriori* Mann-Whitney tests, due to asymmetry of the histological and immunohistochemical data (Sokal & Rolph 1981). Differences were considered significant at $p \leq 0.05$.

3. Results

The total doses absorbed by the earthworms after 7 days of irradiation at 10°C and 10mGy/h was 1.64 ± 0.21 Gy. At 20°C, the total absorbed doses were 0.022 ± 0.003 Gy at 0.135 mGy/h and 1.65 ± 0.22 Gy at 10 mGy/h.

Compared to controls, the results obtained after exposure to ionizing radiation highlighted an increasing apoptotic activity with the received dose within the earthworm tissues, independently of the cell staining method used. Thus, at 10°C, the average number of apoptotic cells (NAC) measured by the TUNEL method, all tissues combined, reached 3.42 ± 2.1 cell.mm⁻² in absence of irradiation, while this average increased to 9.24 ± 3.3 cell.mm⁻² in specimens exposed to 10 mGy.h⁻¹ (figure 7). At 20°C, no significant differences were noticed between the control treatment and an exposure to 0.14 mGy.h⁻¹. The density of apoptotic cells reached

respectively 3.64 ± 2.9 and 3.3 ± 2.5 cell.mm⁻². However, after an exposure to 10 mGy.h^{-1} , cells undergoing apoptotic process increased up to 13.58 ± 3.1 cell.mm⁻² in average. Thus, at both temperatures, 10 mGy.h^{-1} of exposure always lead to a significant increase of the NAC compared to the control or to a lower dose rate. No significant differences were observed between the 2 controls at 10°C and 20°C and the low irradiation at 20°C .

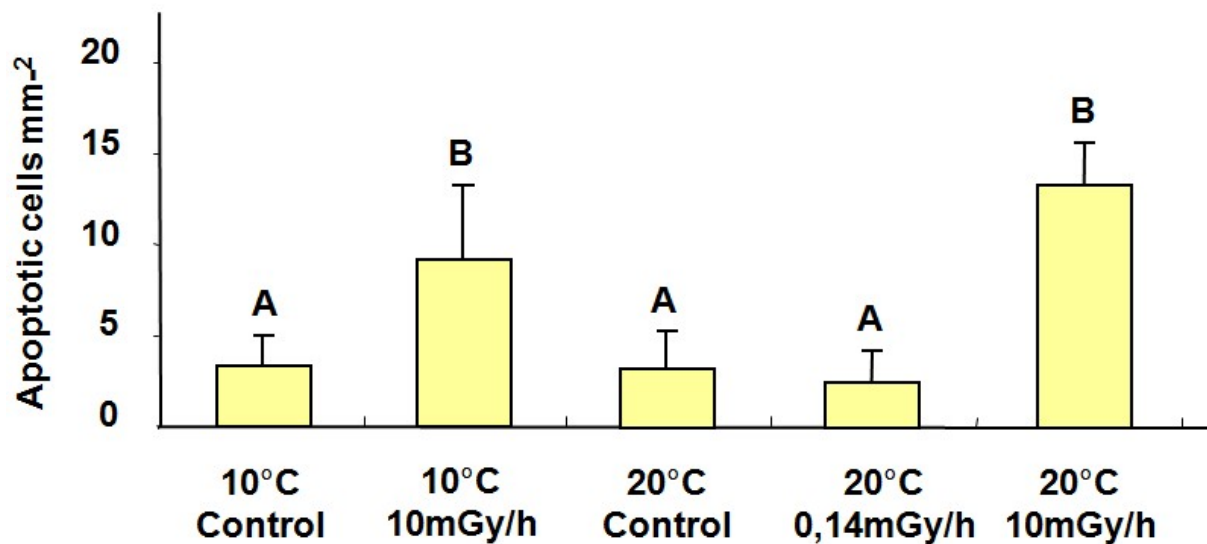


Figure 7: Number of apoptotic cells per mm² measured by TUNEL method and according to exposure temperature and irradiation level (n =5). Results are given all types of tissues combined.

The figure 8 presents a very similar pattern of the apoptotic cell response to the exposure to ionizing radiations, measured by the Apostain method. At 10°C without irradiation, 3.48 ± 1.8 cell.mm⁻² were found undergoing apoptosis. At the same temperature but after exposure to 10 mGy.h^{-1} , this average increased up to 11.34 ± 3.7 cell.mm⁻². At 20°C , 3.58 ± 2.5 apoptotic cell.mm⁻² were found in average for the control treatment, 3.48 ± 2.3 cell.mm⁻² after an exposure at 0.14 mGy.h^{-1} and 12.26 ± 4.4 cell.mm⁻² after an exposure at 10 mGy.h^{-1} . At this irradiation level, the results obtained were always significantly higher ($p \leq 0.01$) compared to the control treatments or the exposure at low dose rate. However, as with the TUNEL method, no significant differences were found between the 3 treatments without irradiation or at low dose rate.

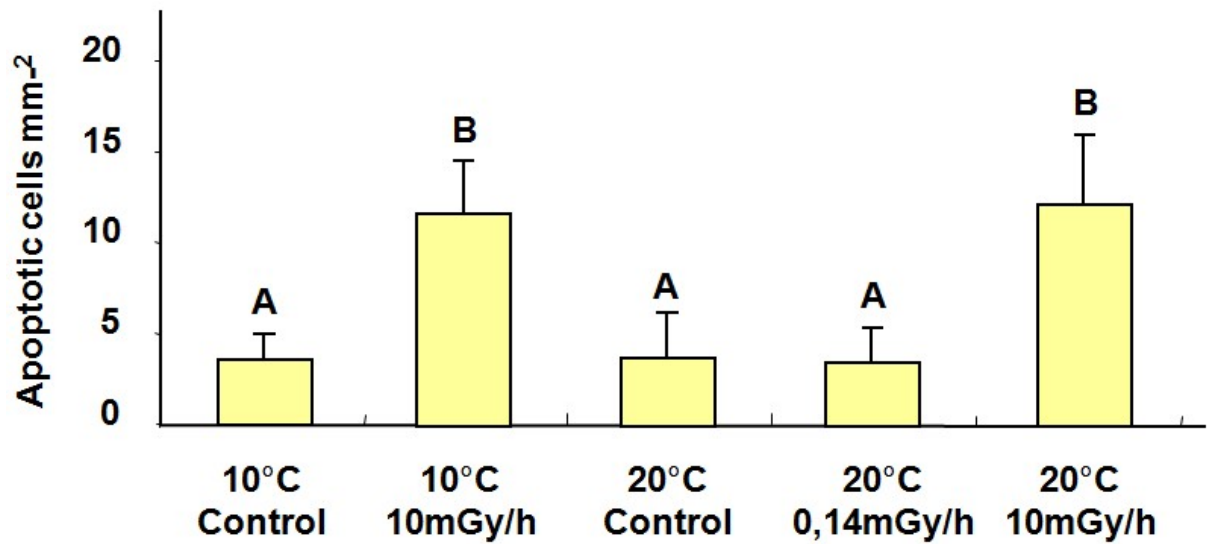


Figure 8: Number of apoptotic cells per mm² measured by Apostain method and according to exposure temperature and irradiation level (n =5). Results are given all types of tissues combined.

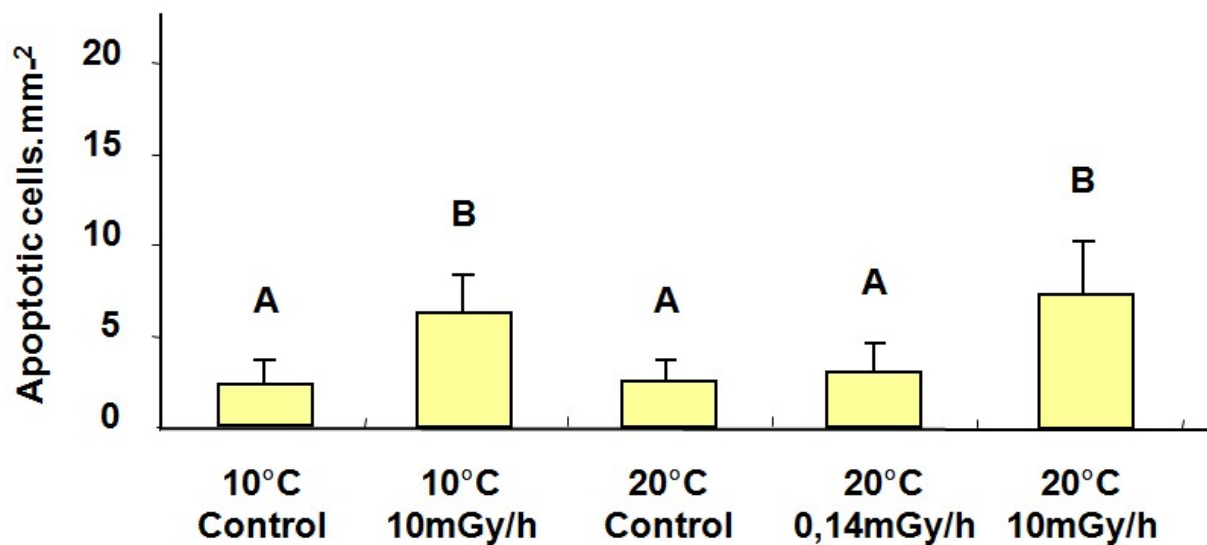


Figure 9: Number of apoptotic cells per mm² measured by the method of caspase 3 detection and according to exposure temperature and irradiation level (n =5). Results are given all types of tissues combined.

The global pattern of the caspase 3 expression followed the tendencies observed with the two previous methods, although the NAC thus brought out was generally lower (figure 9). Indeed,

2.26 +/-0.8 and 2.36 +/-0.3 cell.mm⁻² in average were found undergoing apoptosis for the two control treatments (respectively at 10°C and 20°C) while 6.02 +/-1.2 and 7,36 +/-1.7 cell.mm⁻² could be observed at 10 mGy.h⁻¹, also at same respective temperatures. As before, no statistical differences appeared between controls and low exposure but significant differences were observed between controls or low exposure and high exposures, whatever the considered temperature.

For the 3 used methods, TUNEL, Apostain and caspase 3 detection, no significant differences were visible neither between NAC after exposure to 10 mGy.h⁻¹ nor at 10°C and 20°C. For this level of gamma radiation at 10°C, the TUNEL method revealed 9.24 +/-3.3 apoptotic cell.mm⁻² while 13.58 +/-3.1 cell.mm⁻² were observed at 20°C. Both the Apostain and the caspase 3 detection also showed a very slight increase of the apoptotic activity with the increase of the temperature, but like for TUNEL, neither were statistically significant. Hence, the results indicate a probable absence of temperature effect.

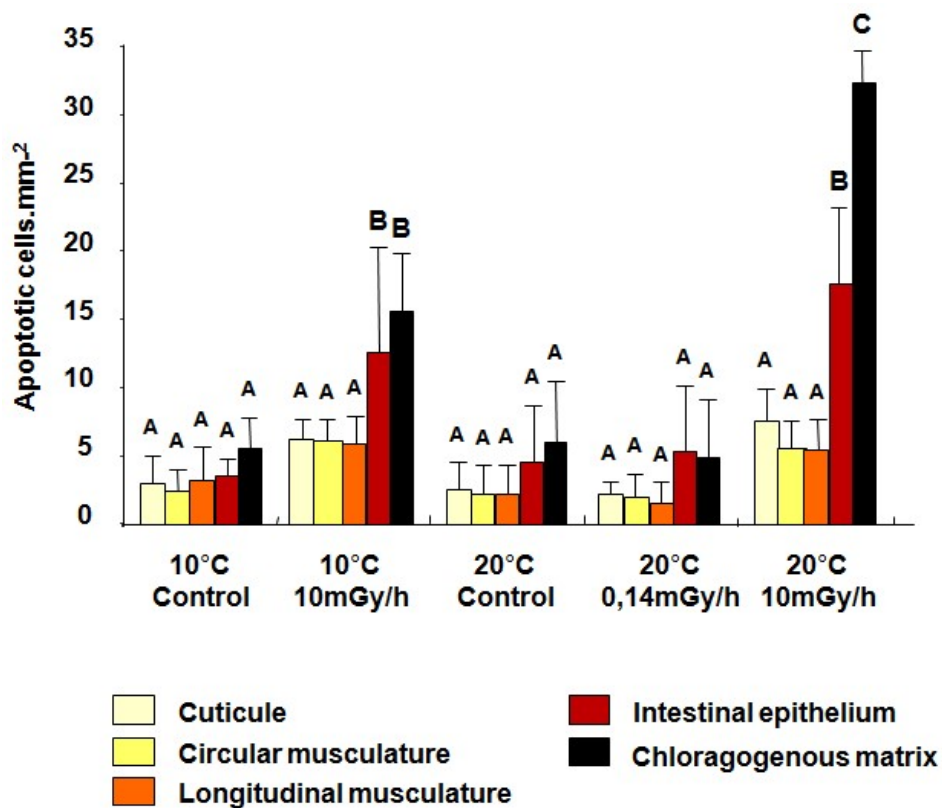


Figure 10: Number of apoptotic cells per mm² measured by TUNEL method and according to exposure temperature and irradiation level. Results are detailed per type of tissue.

When we compared the apoptotic activity between the 5 studied tissues within each treatment, a general pattern appeared. Most of the time, chloragoc and epithelial cells presented a higher activity whatever the treatment (figure 10). After analysis by the TUNEL method, at 10°C and in control (absence of irradiation), between 2.5 +/-1.5 and 3.4 +/-2.4 apoptotic cell.mm⁻² were found within the cuticule and the circular and longitudinal musculatures while 3.2 +/-1.7 and 5.3 +/-2.4 apoptotic cell.mm⁻² were observed, respectively, within the intestinal epithelium and the chloragogenous matrix. At 20°C, again for the control treatment, these values were between 2.3 +/-1.9 and 2.7 +/-1.9 cell.mm⁻² for the cuticule, the circular musculature and the longitudinal musculature, and 4.8 +/-4 and 6 +/-4.5 cell.mm⁻² respectively for the epithelial cells and the chloragogenous tissue. These two latest tissues seemed to present a higher (but not statistically significant) apoptotic background, compared to the cuticule and the two musculatures, at both temperatures. After an exposure to 10 mGy.h⁻¹ of external γ -radiation during 7 days at 10°C, the NAC ranged from 6 +/-1.7 to 6.2 +/-1.3 cell.mm⁻² in average in the cuticule and the two musculatures, 12.6 +/-7.5 cell.mm⁻² ($p \leq 0.01$) in the intestinal epithelium and 15.3 +/-4.5 cell.mm⁻² ($p \leq 0.01$) in the chloragogenous tissue. At 20°C, apoptosis reached 5.2 +/-2.4 to 7.6 +/-2.4 cell.mm⁻² in the cuticule and the musculatures, and 17.2 +/-6 and 32.3 +/-2.7 cell.mm⁻² in respectively the intestinal epithelium and the chloragogenous matrix ($p \leq 0.01$ for both). At both temperatures and after an exposure to 10 mGy.h⁻¹, the NAC had increased by a factor of between 3 and 5 within the epithelium and the chloragogenous matrix. At 10°C there was no difference between these two tissues, but at 20°C the NAC within the chloragoc cells was significantly higher after exposure to 10mGy.h⁻¹. In addition, at 20°C, the exposure to 0.14 mGy.h⁻¹ lead to the same general pattern than described above, although no significant differences were found between tissues. In this treatment, however, slightly less apoptotic cells were found within the chloragoc cells than within the intestinal epithelium.

Figure 11 presents the same results as figure 10, obtained by the TUNEL method, but rearranged per tissue according to the treatment (temperature and irradiation level). With such a rearrangement of the data, Kruskal-Wallis tests and *a posteriori* Mann-Whitney tests highlighted a second general pattern, whatever the type of cell staining method: within a given tissue, an exposure to 10 mGy.h⁻¹ of external γ -radiations during 7 days always lead to an increase of the apoptotic activity. Thus, at 10°C in the cuticule, the NAC increased from

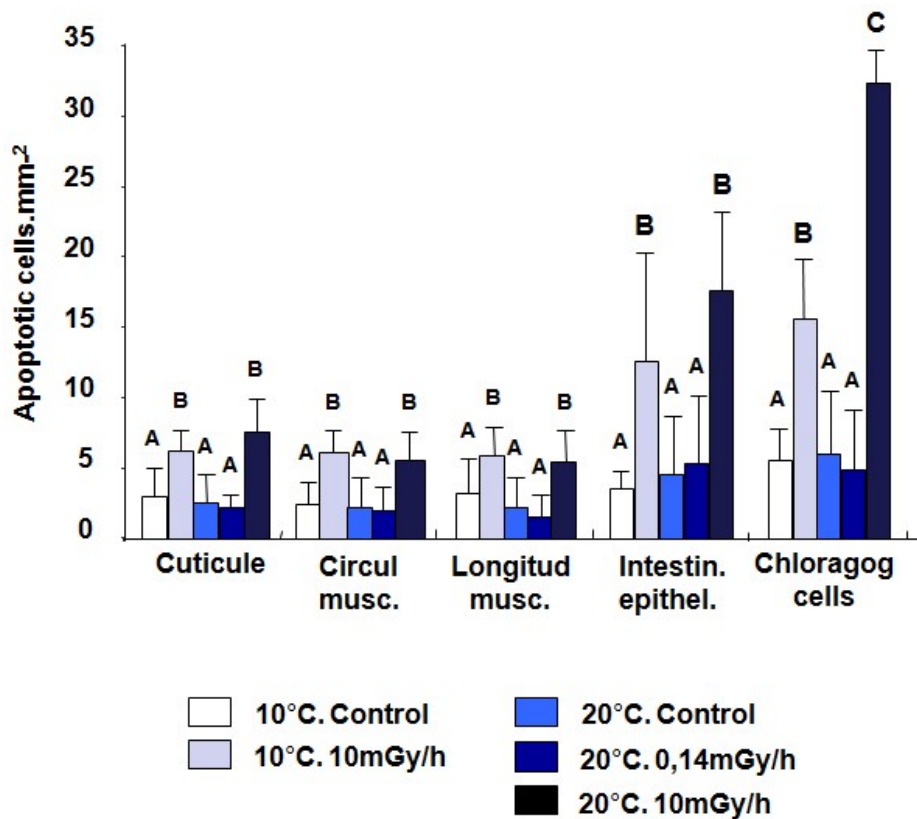


Figure 11: Number of apoptotic cells per mm^2 measured by TUNEL method and according to the type of tissue. Results are detailed per exposure temperature and irradiation level.

2.7 \pm 2.3 to 6.1 \pm 1.5 $\text{cell} \cdot \text{mm}^{-2}$ ($p \leq 0.05$) in average, from the control treatment to an exposure to 10 $\text{mGy} \cdot \text{h}^{-1}$, and from 2.7 \pm 1.9 to 7.6 \pm 2.4 $\text{cell} \cdot \text{mm}^{-2}$ ($p \leq 0.05$) for the same respective exposures at 20°C. In the circular and longitudinal musculatures, the NAC followed the same general pattern. In the epithelial cells and the chloragogenous matrix, these differences became highly significant. Thus, the NAC increased from 3.2 \pm 1.7 to 12.6 \pm 7.5 $\text{cell} \cdot \text{mm}^{-2}$ ($p \leq 0.01$) at 10°C between an absence of irradiation and an exposure to 10 $\text{mGy} \cdot \text{h}^{-1}$, and from 4.8 \pm 4 to 17.2 \pm 6 $\text{cell} \cdot \text{mm}^{-2}$ ($p \leq 0.01$) after the same exposure at 20°C. For the chloragog cells, the obtained values were respectively from 5.3 \pm 2.4 to 15.3 \pm 4.5 $\text{cell} \cdot \text{mm}^{-2}$ ($p \leq 0.01$) at 10°C, and from 6 \pm 4.5 to 32.3 \pm 2.7 $\text{cell} \cdot \text{mm}^{-2}$ ($p \leq 0.01$) at 20°C. No significant differences were found between the two temperatures, except in the chloragogenous tissue exposed at 10 $\text{mGy} \cdot \text{h}^{-1}$, where 15.3 \pm 4.5 $\text{cell} \cdot \text{mm}^{-2}$ at 10°C and 32.3 \pm 2.7 $\text{cell} \cdot \text{mm}^{-2}$ at 20°C ($p \leq 0.01$) were undergoing an apoptotic process. The same tendency was observed within the intestinal epithelium but without statistical significant difference.

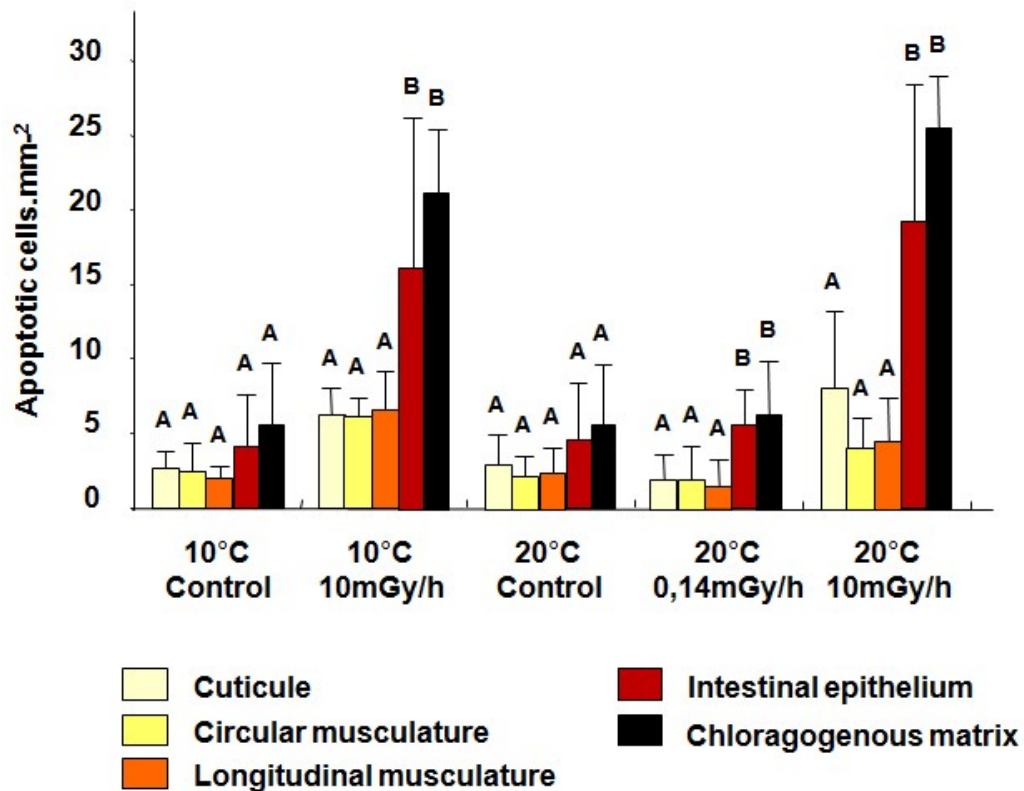


Figure 12: Number of apoptotic cells per mm^2 measured by Apostain method and according to exposure temperature and the irradiation level. Results are detailed per type of tissue.

After cell staining by the Apostain method, the obtained results followed closely those obtained by TUNEL (figure 12). The main differences were a notable higher NAC value within the couple epithelium/chloragogenous tissue at 10°C and $10 \text{ mGy}\cdot\text{h}^{-1}$ and a lower NAC value in the chloragogenous matrix at 20°C and $10 \text{ mGy}\cdot\text{h}^{-1}$. In addition, differences between these two tissues at 20°C and $10 \text{ mGy}\cdot\text{h}^{-1}$ were not significant here, although following the same tendency than with the TUNEL. At 20°C , the exposure to $0.14 \text{ mGy}\cdot\text{h}^{-1}$ presented a pattern similar to the results obtained with the previous method: the NAC value was higher within the couple epithelium/chloragogenous tissue comparing to the three other tissues but, this time, the difference was statistically significant.

When the data were rearranged per tissue according to the treatment (temperature and irradiation level), it appeared again, as with the results obtained by the TUNEL method, that an exposure to $10 \text{ mGy}\cdot\text{h}^{-1}$ always lead to an increase of the apoptotic activity within a given tissue (figures 13 and 14). Thus, at 10°C in the intestinal epithelium, the NAC increased from 4.2 ± 3.4

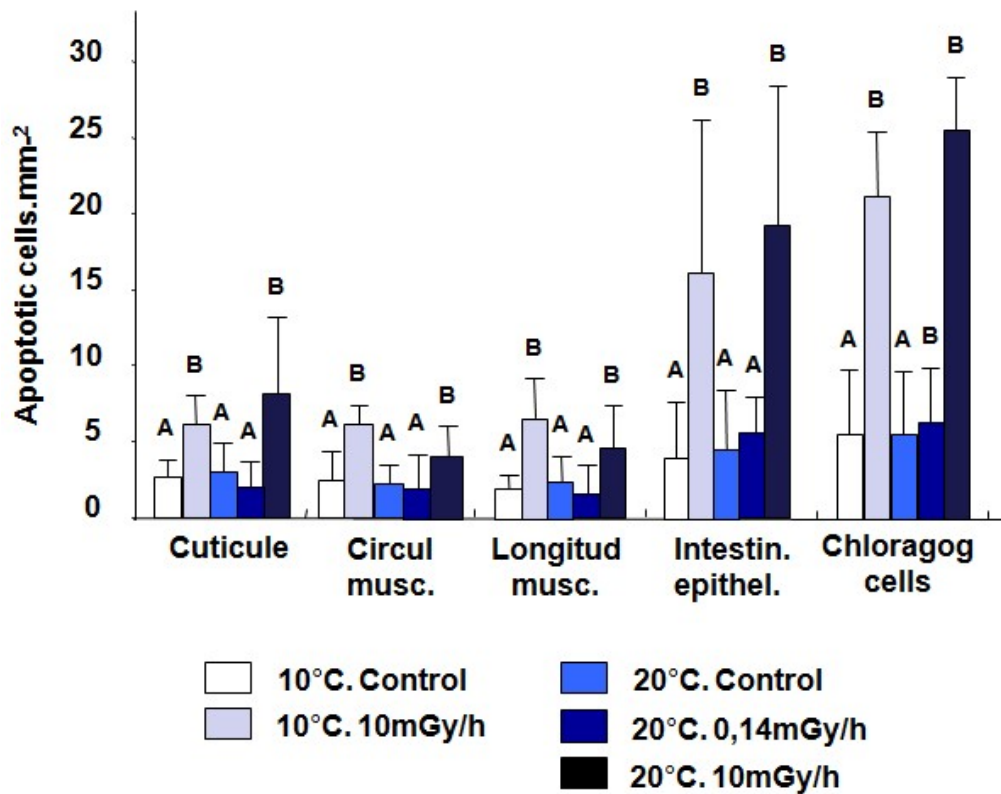


Figure 13: Number of apoptotic cells per mm^2 measured by Apostain method and according to the type of tissue. Results are detailed per exposure temperature and irradiation level.

to $16.9 \pm 9.2 \text{ cell} \cdot \text{mm}^{-2}$ ($p \leq 0.01$) between control and $10 \text{ mGy} \cdot \text{h}^{-1}$, and from 4.5 ± 3.7 to $19.1 \pm 9.1 \text{ cell} \cdot \text{mm}^{-2}$ ($p \leq 0.01$) after the same exposure at 20°C . For the chloragog cells, the obtained values were respectively from 5.3 ± 4.5 to $20.8 \pm 4.4 \text{ cell} \cdot \text{mm}^{-2}$ at 10°C ($p \leq 0.01$), and from 5.5 ± 4.1 to $25.7 \pm 3.3 \text{ cell} \cdot \text{mm}^{-2}$ at 20°C ($p \leq 0.01$). Beyond a tendency of increase in the cuticule, the epithelium and the chloragogenous matrix, no significant differences were found between the two temperatures, thus confirming a low or absence of temperature effect on the apoptosis of earthworm cells after irradiation at this dose level.

The results obtained by detection of the intra-cell caspase 3 activity confirm the global tendencies previously brought out but with a level of apoptosis everywhere lower and slightly different according to the considered tissue (figure 15). Indeed, the higher apoptotic activity previously observed within the epithelium and the chloragogenous matrix was here always statistically significant, including within the controls, but reaching only a maximum of 3.4 ± 0.9

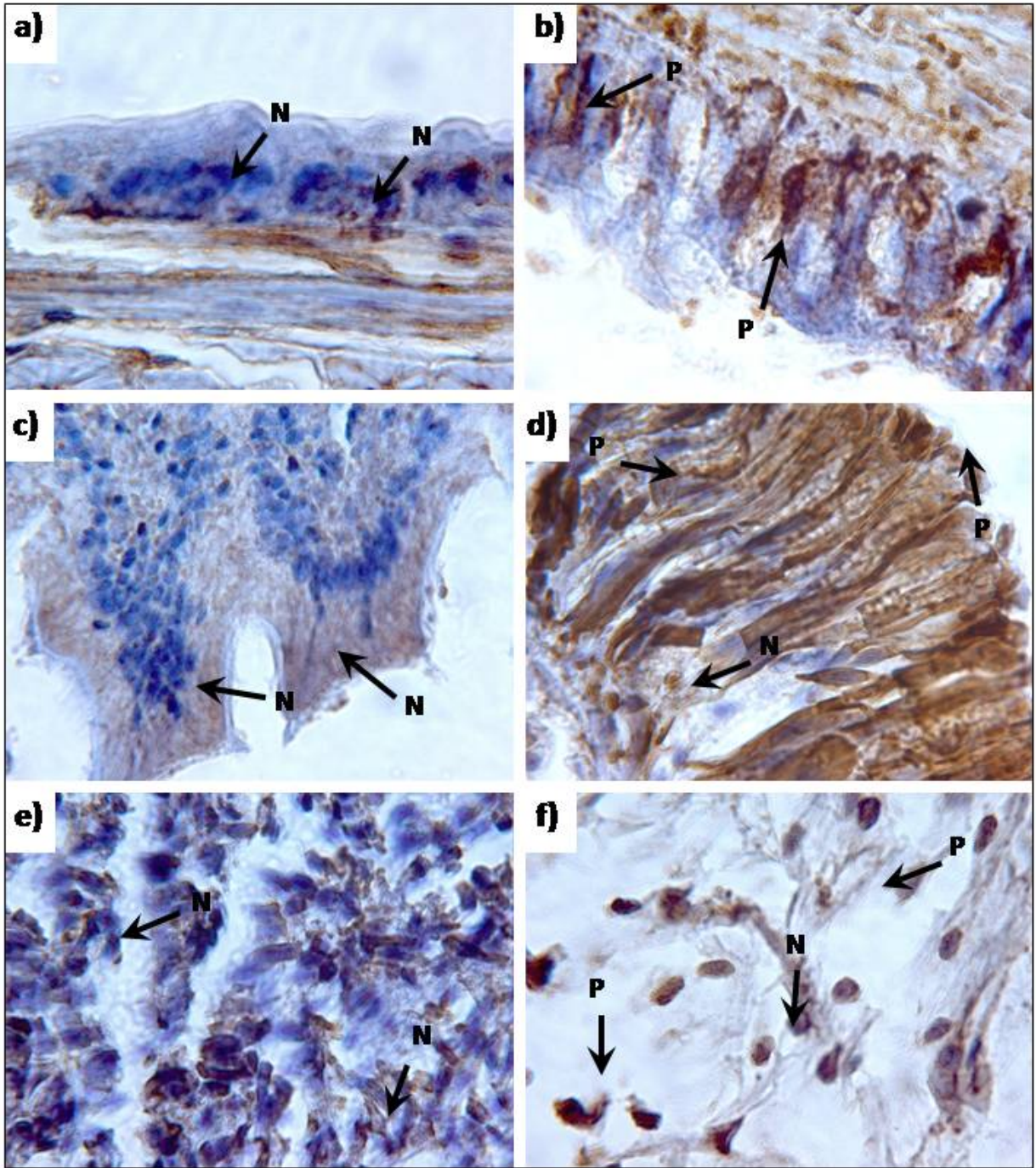


Figure 14: Light microscopy images from Apostain stained tissues (945x magnification) of *Eisenia fetida* exposed to 0 mGy.h⁻¹ (control: plates a, c and e) or 10 mGy.h⁻¹ (plates b, d and f) at 20°C, distinguishing cuticle (a, b), intestinal epithelium (c, d) and chloragogenous tissues (e, f). Arrows indicate negative (N) and positive (P) apoptotic response in stained cells.

cell.mm⁻² in average in the epithelium at the controls of both temperatures. At 10°C and 20°C without irradiation, the NAC within the circular musculature was respectively of 0.4 +/-0.2 and 1.1 +/-0.1 cell.mm⁻² and significantly lower than within the other tissues (*p*≤0.01 for both). At 10°C for control (always without irradiation), the NAC in the longitudinal musculature was not significantly different from the epithelium and the chloragogenous matrix. After exposure at 10 mGy.h⁻¹, the NAC of these two latest tissues reached respectively 8.3 +/-1.3 and 7.4 +/-1 cell.mm⁻² at 10°C and 11.7 +/-1.5 and 8.9 +/-3.1 cell.mm⁻² at 20°C, up to two times more than in the other tissues. No significant differences were found between these two tissues, whatever the treatment, including at 10 mGy.h⁻¹ for both temperatures, although in contrast to the TUNEL and Apostain method the chloragogenous matrix tended towards a lower value compared to the epithelium.

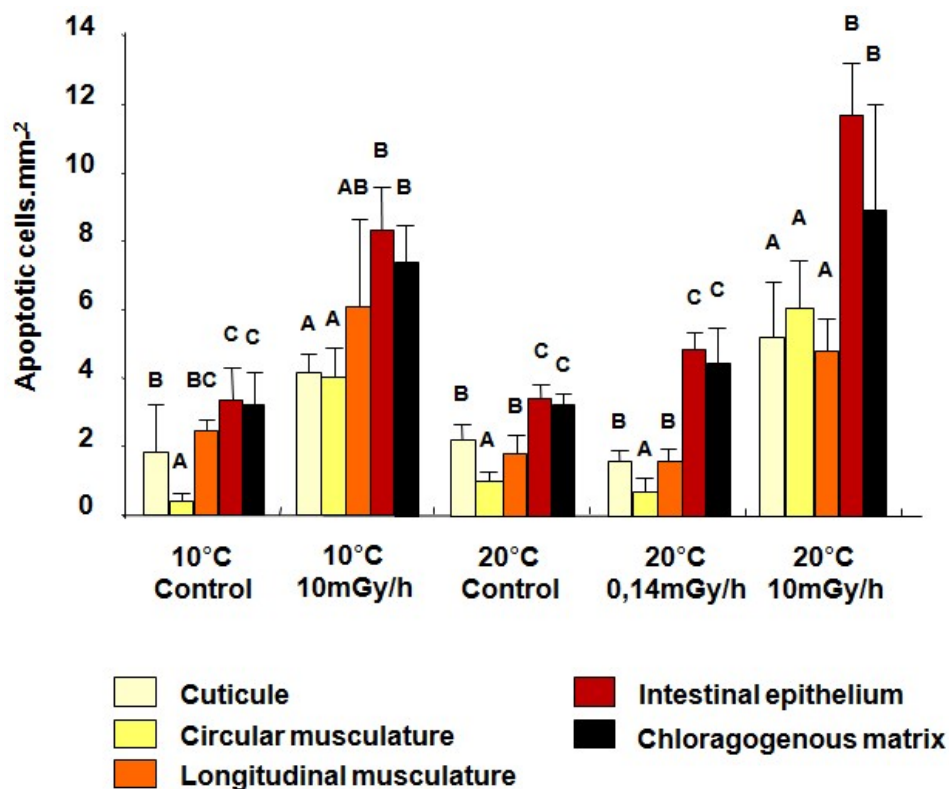


Figure 15: Number of apoptotic cells per mm² measured by the method of caspase 3 detection and according to exposure temperature and irradiation level. Results are detailed per type of tissue.

The increase of the apoptotic activity within the studied tissues associated to an exposure at 10 mGy.h⁻¹, as already described above, was clearly confirmed when data obtained by detection of the caspase 3 activity were rearranged per tissue according to the treatment (figure 16). Like with the previous labeling methods, an increase with exposure was statistically significant for all tissues, sometimes even highly significant in tissues with results usually less pronounced.

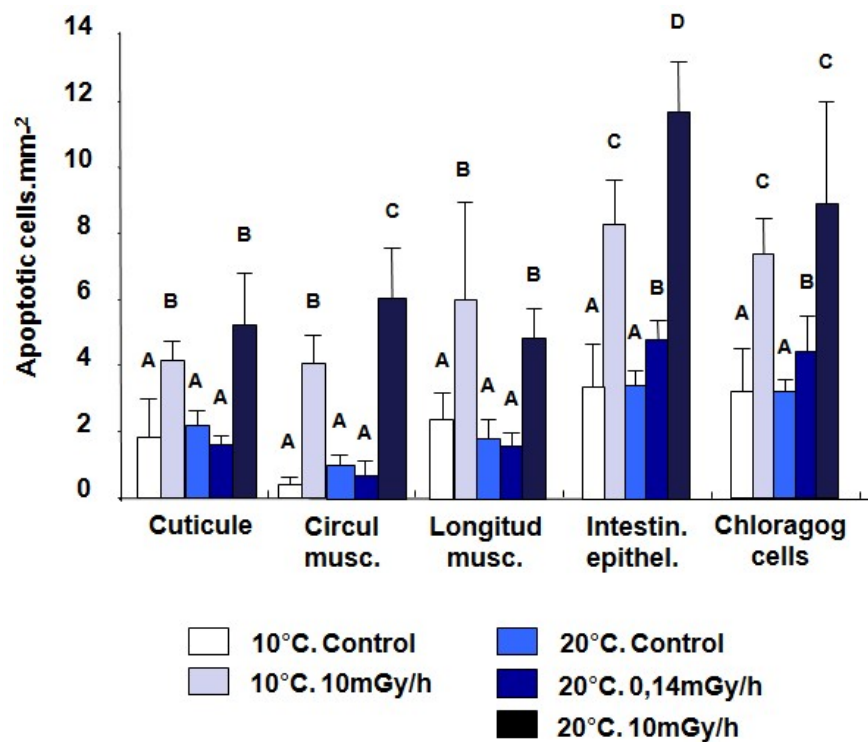


Figure 16: Number of apoptotic cells per mm² measured by the method of caspase 3 detection and according to the type of tissue. Results are detailed per exposure temperature and irradiation level.

Thus, in the circular musculature, the NAC increased from 0.4 +/-0.2 to 4.1 +/-0.8 cell.mm⁻² ($p \leq 0.01$), from control to 10 mGy.h⁻¹ at 10°C, and from 1.1 +/-0.1 to 6 +/-1.3 cell.mm⁻² ($p \leq 0.01$) for the same exposures at 20°C. In the intestinal epithelium exposed at 10 mGy.h⁻¹, the NAC value was of 8.3 +/-1.3 cell.mm⁻² in average at 10°C and up to 11.7 +/-1.5 cell.mm⁻² at 20°C, while in the chloragogenous matrix, these values reached respectively 7.4 +/-1 and 8.9 +/-3.1 cell.mm⁻². Unlike with the two previous methods, epithelial and chloragog cells expressed a higher apoptotic activity when exposed to 0.14 mGy.h⁻¹ at 20°C (respectively 4.9 +/-0.3 and 4.5 +/-0.8 cell.mm⁻²) compared to the corresponding controls (respectively 3.4 +/-0.4 and 3.2 +/-0.4

cell.mm⁻²). Comparing exposures to 10 mGy.h⁻¹ at 10°C and 20°C, tissues showed a tendency for increasing NAC at the higher temperature, with significant differences for the circular musculature and the intestinal epithelium. By consequence, a slight or irregular effect of the temperature on the apoptotic response of earthworms to ionizing radiations could be inferred or suspected, unlike the two previous staining methods.

3.1. Comparison of methods

Beyond similar global tendencies and patterns of apoptotic responses obtained by the three tested methods, differences remain, sometimes significant in terms of statistical analysis (figure 17). Thus, if we consider all the studied tissues combined, a general tendency of lower NAC was brought out by the method of intra-cell caspase 3 detection. This result was significant after exposure to 10 mGy.h⁻¹ at 10°C and 20°C. Indeed, at 10°C, Apostain gave 11.34 +/-3.7 apoptotic cell.mm⁻² while the caspase 3 staining labeled 6.02 +/-1.2 cell.mm⁻² ($p \leq 0.01$). At 20°C, TUNEL brought out 13.58 +/-3.1 apoptotic cell.mm⁻² and the caspase 3 method only 7.36 +/-1.7 cell.mm⁻² ($p \leq 0.01$).

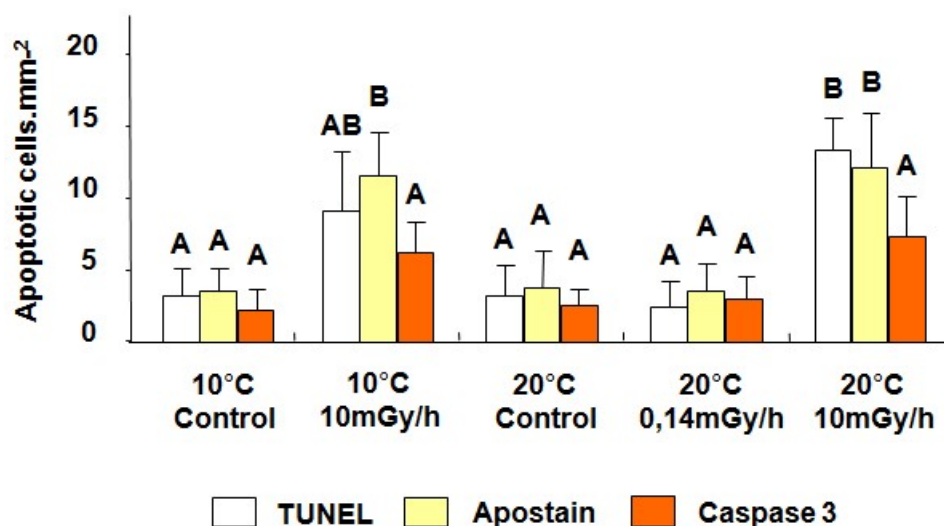


Figure 17: Comparison of the results obtained by the 3 staining methods (in number of apoptotic cells per mm²) according to exposure temperature and irradiation level.
What tissue? (n=)

4. Discussion

This study constitutes, together with parallel works within our team (Lapied et al. 2010, 2011), one of the very first reports and descriptions of the apoptotic process in earthworms. In addition, our results has demonstrated the applicability of apoptosis as a useful and reliable biomarker for radiation impacts in these organisms. Three major results were highlighted: 1) within a given tissue, an exposure to $10 \text{ mGy}\cdot\text{h}^{-1}$ of external γ -radiations during 7 days always led to an increase of the number of apoptotic cells compared to the controls; 2) in all groups the intestinal epithelium and the chloragogenous matrix, and in a very lower extent the cuticule, showed a higher level of apoptosis compared to other tissues and 3) the temperature had probably low or no effects on the results between 10°C and 20°C .

4.1. Inter-comparison between the methods

The three different staining methods used gave comparable results although notable differences should be considered. Globally, even if the most often not statistically significant, a lower number of apoptotic cells was found with the caspase 3 labeling method, whatever the temperature and the level of irradiation (figure 11). This difference became even significant at $10 \text{ mGy}\cdot\text{h}^{-1}$ for both temperatures. In addition, the apoptotic activity revealed by this method in the muscular tissues showed also notable differences. For instance, a particularly low level, in relative data by comparison with the other tissues, was observed in the circular musculature at 10°C in the controls (without irradiation) and an unusual high level at 10°C and $10 \text{ mGy}\cdot\text{h}^{-1}$ in the longitudinal musculature. Moreover, the caspase 3 labeling method was the only one that showed a statistically significant increase at only $0.14 \text{ mGy}\cdot\text{h}^{-1}$ in 7 days (figure 12). This result is of strong interest considering the central role of caspase 3 in the control of the apoptotic cascade, in particular as a molecule regulated by mitochondria through the release of cytochrome c, as already mentioned above. The possible improved sensitivity of this method compared to TUNEL and Apostain might reflect the relatively lower background levels in controls.

Beyond an unavoidable level of incertitude linked in any type of molecular analysis method, including the immunohistochemical techniques, the obtained variations in our results may have

several sources. TUNEL, Apostain and caspase 3 labelling do not target the same step within the apoptotic cascade. In particular, TUNEL detects cells in last phase of apoptosis while Apostain stains cells according to their chromatin texture during the early phase of the process. Thus, the fact that all apoptotic cells are not at the same step at the same time may explain, at least partially, the obtained results. Another possible source of variation could be a possible expression of caspase 3 in other cell processes than apoptosis. Indeed, if this molecule occupies a central position in the apoptotic cascade, it has been shown that caspases, including caspase-3, are involved in cell processes other than apoptosis. Thus, caspase-3 may play a role in hematopoietic stem cell differentiation (Abdul-Ghani & Megeney 2008). In addition, while TUNEL became worldwide massively used in the 1990s and the 2000s, a debate about its accuracy arose when necrotic cells were found to be inappropriately labeled as apoptotic (Grasl-Kraupp et al. 1995). Since then, the method has been improved and has largely demonstrated its efficiency (Negoescu et al. 1996, 1998).

Considering our results and the mechanisms of action of the three tested staining methods, caspase 3 labeling seems to be a particularly efficient method in detecting apoptotic cells although, as far as possible, it should always be associated with other complementary methods. In addition, unlike TUNEL and Apostain which are designed to target specific DNA breaks or strands, caspase 3 labeling targets a molecule directly involved in the apoptotic cascade.

4.2. Tissue apoptotic response

The general apoptotic response of earthworms to stress from ionizing radiation can be put in parallel with the result obtained by Lapied et al. (2010) after an exposition of earthworms to silver nanoparticles. Both ionizing radiation and nanoparticles gave a response in the intestinal epithelium and chloragogenous matrix. However, the cuticule, tissue being the most at the interface between the external and the internal environment and thus, the most exposed to potential external aggressions, was not significantly affected by external ionizing radiations when compared to the other tissues. When exposed to silver nanoparticles, this tissue barrier was as affected as the epithelial and the chloragogenous cells (Lapied et al. 2010). At the opposite, circular and longitudinal musculatures seemed to have a lower apoptotic response to the irradiation since the apoptotic activity was not significantly different when compared to the

most sensitive tissues, whatever the level of exposure. Globally, with the exception of the cuticle, the apoptotic response of the four other studied tissues followed, after exposure to ionizing radiations, a pattern similar to the one obtained after contamination by nanoparticles.

Thus, disturbances in the cell functioning observed at $10 \text{ mGy}\cdot\text{h}^{-1}$ might indicate, in a first approximation, a notable radiosensitivity of the intestinal epithelium, the chloragogenous matrix and, although less evident, possibly the cuticle and the muscular structures in earthworms. However, the significance of an apoptosis stimulation or over-activation, in terms of radiosensitivity, remains to be clarified. Indeed, Azria et al. (2014) recently established in human a reverse correlation between the rate of radio-induced apoptosis in lymphocytes and the radiosensitivity of patients after radiotherapy (very high doses received). The higher was the apoptotic response in lymphocytes, the higher was the radio-resistance of patients. In addition, after previous dose-response experiments carried out in our laboratory with fish exposed to Uranium, the apoptotic signal increased with dose rate (total dose) until high exposure where the apoptotic signal disappeared. At this point, it seemed that the apoptotic system was compromised.

To date, mechanisms at the origin of these results remain unsolved. However, it must be concluded that high radio-induced apoptosis is not necessarily synonym with radiosensitivity or radioresistance. We can infer that, beyond a threshold which remains to be determined (probably below 10 mGy/hr), such an over-activation of the apoptotic process in tissues, in particular in vital tissue structures, probably triggers an energetic over-cost with potential heavy consequences on the organism physiology. As described above, the cuticle is an external integument protecting the entire body against abrasion and constitutes the first barrier against external potential aggressions. The intestinal epithelium plays a central role in the ingested soil transit, the absorption of nutrients and the establishment of a mutualistic intestinal microbiota and the chloragogenous tissue, covering the external pared of the intestine is a crucial organ playing a great role in the ionic regulation and the structuring of the immune system through the production of chloragocytes and antibacterial molecules. Potential damages or an over-stimulation of the apoptotic activity resulting in an irradiation, as observed in this work, might affect numerous crucial cell and physiological processes controlled by these three tissue structures.

4.3. Ecosystem relevance

Assessing the effects of irradiations on soil invertebrate models has two objectives: at the species and individual scale, to better understand the toxicological response, and at the environmental scale, to better understand the ecosystemic response. Although representative of a relatively high dose rate, $10 \text{ mGy}\cdot\text{h}^{-1}$, and a dose rate at which significant detrimental effects have been demonstrated in earthworm reproduction, the highest level of exposure in this work, corresponds to a relatively low total dose (1.65 Gy) compared to toxicological tests carried out in most investigations on earthworms and levels measured in contaminated fields. However the results could suggest that the apoptotic response can represent an early warning of potential detrimental effects, and would be a useful biomarker for both exposure and effects.

Thus in laboratory, Hancock (1962) reported that, after having exposed *Lumbricus terrestris*, to acute ionizing radiations, no lethal effect occurred at 45 kRad (450 Gy) or below. The mortality began to appear with 75 kRad (750 Gy), when the LD50 in mammals is usually around 0,5 kRad (5 Gy). All the worms died within 2 months after 100 kRad (1000 Gy). *Eisenia fetida*, a routinely used species in ecotoxicological works, has been studied by several authors in the frame of radiological tests. Thus, in an acute exposure experiment, Suzuki & Egami (1983) showed that 20 Gy had no apparent effect on growth and maturation of the juveniles, while these processes were inhibited at 100 Gy. Wilding et al., in 2006, studied the mitochondrial DNA (mtDNA), known to exhibit an increased mutation rate after exposure to ionizing radiations. They observed a significant elevation in mtDNA mutation frequency at 8.5 mGy/h (total dose 11.22 Gy and mutation frequency: $27.98 \pm 4.85 \times 10^{-5}$ mutations/bp) in comparison to controls without irradiation (mutation frequency: $12.68 \pm 3.06 \times 10^{-5}$ mutations/bp). In parallel, no elevation in mutation frequency was seen at 1.4 mGy/h, the lower dose rate (total dose 1.85 Gy; mutation frequency: $13.74 \pm 1.9 \times 10^{-5}$ mutations/bp) compared to controls.

From 2007, Hertel-Aas et al. showed that an adaptation or, at least, a stabilization of the reproduction capacities could occur in the earthworm species model *Eisenia fetida* (Hertel-Aas et al. 2007; Hertel-Aas et al. 2011). These authors exposed *Eisenia fetida* to ^{60}Co radiation during two consecutive generations, at dose rates from 0.18 to 43 mGy/h. After 13 weeks at 43

mGy/h, no radiation-induced effect on the cocoon production rate by adults of the first generation was notable, neither by adults of the second generation after another 13 weeks of exposure. However, the hatchability of cocoons produced by the first generation during the first 4 weeks was reduced to 60 % at 43 mGy/h, and no cocoons produced after 5-13 weeks hatched. At 11 mGy/h, the hatchability of the cocoons produced after 9-13 weeks was reduced to 25 %. The number of hatchlings per hatched cocoon was also reduced at both 11 and 43 mGy/h. For adult individuals of the second generation, hatchability of cocoons produced and number of hatchlings per cocoon (individuals of third generation) was also reduced (up to almost 70 % for the hatchability) during the 13-week of exposure. However, the hatchability increased with time, suggesting a possible adaptation of individuals from the second generation. In another study, the same author (Hertel-Aas et al. 2011) found that a sub-chronic exposure at 17 mGy/h (accumulated dose: 25 Gy) induced a temporary sterility in *Eisenia fetida*, recovered after 8 weeks.

The earthworm resistance to radioactivity may depend on various parameters, including the type of radiation and some environmental factors. Thenceforth, this capacity is not always evident (Jackson 2005). In experiments with ^{90}Sr , ^{137}Cs , ^{106}Ru , ^{95}Zr , ^{65}Zn , ^{125}Sb and ^{239}Pu on various groups composing the soil fauna, earthworms and Myriapods (Diplopods and Chilopods) appeared to be the most affected (Krivolutskii 1987). The authors inferred that this result was probably due to the fact that these organisms are in close contact with soil elements, consuming decaying plant litter and dwelling mainly in the upper soil layers, where the bulk of radionuclides is accumulated. He also noted a particular sensitivity in earthworms to an increased Ra radiation background and concluded, considering all these elements, that these animals are among the best bioindicators of polluted soils.

In the field, several authors investigated the impact of ionizing radiations on the soil fauna, and particularly on earthworms, in areas contaminated by radionuclides, such as around the Chernobyl nuclear power plant, in Ukraine. Following the reactor accident in April 1986, about 3-4 tons of U fuel including 3 to $6 \cdot 10^5$ TBq ^{137}Cs and 2 to $4 \cdot 10^5$ TBq ^{90}Sr were released to the atmosphere (Jackson 2005). More than half of that released was deposited within the 30 km zone around the site, leading to a great tree mortality and the establishment of a human exclusion zone. At heavily contaminated sites, juvenile earthworms did not survive or hatched

from cocoons during the autumn 1986, although adults produced cocoons during this period (Krivolutsky & Pokarzhevsky, 1992). In the first year after the accident, the abundance of earthworms reached only 15 % of the abundance found in a non-contaminated control site, but they reproduced and produced cocoons even in the most contaminated areas (Sokolov et al. 1994). After 2.5 years, the soil fauna was almost entirely restored in density, but not in diversity. Even 10 years after the accident, the diversity represented only 80 % of the one before the accident (Krivolutsky 1996).

In Russia, near the Ural mountains (North of the Perm oblast), 45-kilotons of nuclear explosive (PNE) were fired underground on the 23rd of March 1971, as a preliminary step to build a water canal between the Pechora River basin (Komi Republic), through the Kama and Volga rivers, to the Caspian Sea. After the explosion, the density and relative abundance of the earthworm species *Eisenia nordenskioldi* were compared between two contaminated sites, where the background level of radiations varied from 0.7 to 2.43 $\mu\text{Gy}\cdot\text{h}^{-1}$ (80 to 280 $\mu\text{R}\cdot\text{h}^{-1}$), and a control site, with a background level at 0.1-0.16 $\mu\text{Gy}\cdot\text{h}^{-1}$ (12-18 $\mu\text{R}\cdot\text{h}^{-1}$) (Kolesnikova et al. 2005). In the two contaminated sites, the density of *E. nordenskioldi* was 3.2 $\text{ind}\cdot\text{m}^{-2}$ and 0,8 $\text{ind}\cdot\text{m}^{-2}$, corresponding to a relative abundance of respectively 5.6 % and 1.9 %. In the control, the density was 1,8 $\text{ind}\cdot\text{m}^{-2}$ with a relative abundance of 1-3 %.

In Siberia, Gongalsky (2003) found that the abundance and biodiversity of soil macroinvertebrates was 3 to 37 times lower in a site contaminated by uranium production and concluded that this type of contamination has severe negative biological effects on key groups of the soil food web. It should be noticed here that, as with the results obtained by Kolesnikova et al. (2005) in Russia, these effects could be due both to irradiation and metal accumulation in biological tissues, thus demonstrating potential consequences of multiple stressors.

Thus, we can conclude from these results that earthworms, although more radio-resistant than mammals, as most invertebrates (UNSCEAR 2008), appear to be among the most radiosensitive component of the soil fauna. However, this sensitivity seems to be dependent on the stage of development, immatures and juveniles being more radiosensitive than adults as also seen for other organisms. In addition, results obtained in previous works combined with our own results tend to show that, at a dose corresponding to a reduction of cocoon hatchability, ionizing

radiations trigger an apoptotic response in tissues constituting the major part of the animal body.

4.4. Effect of Temperature

In nature, most earthworm species enter in diaposis during a part of the year. This form of dormancy occurs particularly when the temperatures fall down beyond a certain threshold, during the winter in boreal and temperate countries, or when the drought reach an intolerable level, in Mediterranean and dry tropical areas. Below the physiological optimal temperature and before reaching the temperature of diaposis, the worm activities begin to slow down its metabolic activity but still stay functional. *E. fetida*, which is a common epigeic species in temperate climates, is still active at 10°C, although having a slower metabolism. In our experiment, the apoptotic activity followed a similar pattern whatever the temperature of exposure. Except at 20°C and after an exposure at 10 mGy.h⁻¹, where the number of apoptotic cells was significantly higher in the chloragogenous matrix than in the intestinal epithelium obtained with the TUNEL method, the three staining techniques provided comparable data. Beyond to enhance the robustness of our results, it underlines also the reliability of these three approaches. This result demonstrates that far from its optimal level of temperature (20°C), and even with a slowed metabolism, this species is still strongly affected by ionizing radiations. Transferred to the nature where most epigeic species of a given temperate area follow similar patterns of behaviour regarding the temperature and the seasons, this result allows to hypothesize that most temperate earthworm species could stay sensitive to ionizing radiations a great part of the year, not only during the optimal environmental conditions.

These considerations and our results suggest that to assess the impact of ionizing radiations on earthworms, and more generally on invertebrates, via immunohistochemical techniques, combining several methods is recommended as already mentioned above, and particularly methods targeting different steps of the apoptotic cascade. TUNEL and Apostain assays and caspase 3 labeling, with a relatively low and comparable cost, are a good alternative despite long experimental settings.

4.5. Conclusions and future work

Both Lapied et al. (2010) and this work clearly showed that the apoptotic answer after contamination by nanoparticles or irradiation considerably varies from a tissue type to another, However, the reasons of this difference of cell behaviour and the underlying mechanisms remain unsolved. In the future, complementary methods could be used to try to clarify these processes. Thus, combined with immunohistological methods allowing to visualize and map the distribution of the apoptotic cells within a tissue section, gene expression could be analyzed through transcriptomic methods. This approach may strongly contribute to determine the fine processes acting within the cells during and after an exposure to ionizing radiations. Such new generation methods could be now applied to earthworms since the genome sequencing of a first earthworm species, *Lumbricus rubellus*, is achieved (Stürzenbaum et al. 2009) and that of *E. fetida* is about to be completed. Moreover, the tendency of NAC increase with the temperature observed in this work, although not significant, could justify a repeat of this study with more samples and a method with higher resolution, and at a higher dose rate to obtain a dose-effect relationship.

In addition, very few studies have demonstrated to date the existence of caspase-like proteins in earthworms. In 2007, Homa et al. showed an upregulation of caspase 3 in *Allolobophora chlorotica* and *Eisenia fetida* after exposure to Cu, Pb and Cd, while this result was not obtained after exposure to Zn. Thus, the present study constitutes a pioneer work in showing the conservation of caspase 3 or caspase 3-like proteins in earthworms and, thus, the impact of ionizing radiations on its main regulators: mitochondria and its production of cytochrome c.

E. fetida is, by far, the most widespread used earthworm model in ecotoxicological studies. As epigeic species living within the litter and the soil organic matter, it represents, however, only a fraction of the ecological categories of earthworms living in the nature. It may have ecological and physiological behaviors different from anecic or endogeic species, the two other main ecological categories of earthworms, living deeper in the soil and respectively coming up or not to the surface to feed. Thus, comparing two or several species of different ecological categories may help in transferring experimental results from the laboratory to the field.

5. References

- Ameisen, J.C. 1996. The Origin of Programmed Cell Death. *Science*, 272, 5266, 1278-1279.
- Aravind, L., Dixit, V.M. & Koonin, E.V. 1999. The domains of death: evolution of the apoptosis machinery. *TIBS*, 24, 47-53.
- Bigorgne, E., Foucaud, L., Lapied, E., Labille, J., Botta, C., Sirguy, C., Falla, J., Rose, J., Joner, E.J., Rodius, F. & Nahmani, J. 2011. Ecotoxicological assessment of TiO₂ byproducts on the earthworm *Eisenia fetida*. *Environmental Pollution*, 159: 2698-2705.
- Brown, G.G. 1995. How do earthworms affect microfloral and faunal community diversity ? *Plant and Soil*, 170, 209-231.
- Brown, S.L. & Bell, J.N.B. 1995. Earthworms and radionuclides, with experimental investigations on the uptake and exchangeability of radiocaesium. *Environmental Pollution*, 88: 21-39.
- Bunzl, K. 2002. Transport of fallout radiocesium in the soil by bioturbation: a random walk model and application to a forest soil with a high abundance of earthworms. *The Science of the Total Environment*, 293: 191-200.
- Cancio, I., Gwynn, I., Ireland, P.M. & Cajaraville, M.P. 1995. Lysosomal origin of the chloragosomes in the chloragogenous tissue of the earthworm *Eisenia foetida*: cytochemical demonstration of acid phosphatase activity. *Histochem. J.*, 27, 591-596.
- Cooper, E.L. & Roch, P. 1992. The capacities of earthworms to heal wounds and to destroy allografts are modified by polychlorinated biphenyls (PCB). *J. Invertebr. Pathol.*, 60, 59-63.
- Coutris, C., Hertel-Aas, T., Lapied, E., Joner, E.J. & Oughton, D.H. 2011. Bioavailability of cobalt and silver nanoparticles to the earthworm *Eisenia fetida*. *Nanotoxicology*, 6 (2): 186-195.
- Dales, R.P. & Kalaç, Y. 1992. Phagocytic defense by the earthworm *Eisenia foetida* against certain pathogenic bacteria. *Comp. Biochem. Physiol.*, 101A, 487-490.
- Edwards, C.A. & Bohlen, P.J. 1996. *Biology and Ecology of Earthworms*. Chapman and Hall, London (ed.), 440 pp.
- Espinoza-Navarro, O. & Bustos-Obregón, E. 2005. Effect of malathion on the male reproductive organs of earthworms, *Eisenia foetida*. *Asian J Androl*, 7 (1), 97-101.
- Estabel, J., Mercer, A., König, N. & Exbrayat, J.M. 2003. Programmed cell death in *Xenopus laevis* spinal cord, tail and other tissues, prior to, and during, metamorphosis. *Life Sciences*, 73 (25), 3297-3306.
- Fayolle, L., Michaud, H., Cluzeau, D. & Stawiecki, J. 1997. Influence of temperature and food source on the life cycle of the earthworm *Dendrobaena veneta* (Oligochaeta). *Soil Biology and Biochemistry*, 29(3-4): 747-750.

- Ferlini, C., Kunkl, A., Scambia, G. & Fattorossi, A. 1997. The use of Apostain in identifying early apoptosis. *J. Immunol. Meth.* 205, 95-101.
- Fesenko, S.V., Alexakhin, R.M., Geras'kin, S.A., Sanzharova, N.I., Spirin, Ye.V., Spiridonov, S.I., Gontarenko, I.A. & Strand, P. 2005. Comparative radiation impact on biota and man in the area affected by the accident at the Chernobyl nuclear power plant. *Journal of Environmental Radioactivity*, 80: 1-25.
- Fischer, E. & Trombitás, K. 1980. X-ray microprobe analysis of chloragosomes of untreated and of EDTA-treated *Lumbricus terrestris* using fresh air-dried smears. *Acta histochemica*, 66, 237-242.
- Frankfurt, O.S. & Krishan, A. 2001. Identification of apoptotic cells by formamide-induced DNA denaturation in condensed chromatin. *J. Histochem. Cytochem.* 49, 369–378.
- Fritsch, C., Scheifler, R., Beaugelin-Seiller, K., Hubert, P., Coeurdassier, M., De Vaufleury, A. & Badot, P.M. 2008. Biotic interactions modify the transfer of cesium-137 in a soil-earthworm-plant-snail food web. *Environmental Toxicology and Chemistry*, 27 (8): 1698-1707.
- Geras'kin, S.A., Evseeva, T.I., Belykh, E.S., Majstrenko, T.A., Michalik, B. & Taskaev, A. 2008. Effects on non-human species inhabiting areas with enhanced level of natural radioactivity in the north of Russia: a review. *J. Environ. Radioact.*, 94: 151–82.
- Gongalsky, K.B. 2003. Impact of pollution caused by uranium production on soil macrofauna. *Environmental Monitoring and Assessment*, 89: 197–219.
- Hancock, R.L. 1962. Lethal doses of irradiation for *Lumbricus*. In *Life Sciences*, pp. 625–628. Pergamon-Elsevier Science Ltd, Oxford.
- Hertel-Aas, T., Oughton, D.H., Jaworska, A., Bjerke, H., Salbu, B. & Brunborg, G. 2007. Effects of chronic gamma irradiation on reproduction in the earthworm *Eisenia fetida* (Oligochaeta). *Radiat. Res.*, 168: 515–526.
- Hertel-Aas, T., Oughton, D.H., Jaworska, A. & Brunborg, G. 2011. Induction and repair of DNA strand breaks and oxidised bases in somatic and spermatogenic cells from the earthworm *Eisenia fetida* after exposure to ionising radiation. *Mutagenesis*, 26: 783-93.
- Hertel-Aas, T., Brunborg, G., Jaworska, A., Salbu, B. & Oughton, D.H. 2011. Effects of different gamma exposure regimes on reproduction in the earthworm *Eisenia fetida* (Oligochaeta). *Science of the Total Environment*, 412-413: 138-47.
- Holmstrup, M. 2003. Overwintering adaptations in earthworms. *Pedobiologia*, 47: 504-510.
- Hønsi, T.G. & Stenersen, J. 2000. Activity and localisation of the lysosomal marker enzymes acid phosphatase, N-acetyl- β -Dglucoaminidase, and β -galactosidase in the earthworms *Eisenia fetida* and *E. veneta*. *Comp. Biochem. Physiol.*, 125B, 429–437.

- Ireland, M.P. & Fisher, E. 1978. Effect of Pb^{2+} on Fe^{3+} tissue concentrations and delta-amino-laevulinic acid dehydratase activity in *Lumbricus terrestris*. *Acta biologica Academiae scientiarum hungaricae*, 29, 395-400.
- Jackson, D., Copplestone, D., Stone, D.M. & Smith, G.M. 2005. Terrestrial invertebrate population studies in the Chernobyl exclusion zone, Ukraine. *Radioprotection*, 1 (40): 857-863.
- Jamieson, B.G.M. 1981. *The Ultrastructure of the Oligochaeta*. Academic Press Inc., London, 462 pp.
- Jones, C.G., Lawton, J.H. & Shachak, M. 1994. Organisms as ecosystem engineers. *Oikos*, 69 (3): 373-86.
- Kolesnikova, A.A., Taskaeva, A.A., Krivolutskii, D.A. & Taskaev, A.I. 2005. Condition of the Soil Fauna near the Epicenter of an Underground Nuclear Explosion in the Northern Urals. *Russian Journal of Ecology*, 36 (3): 150–157.
- Krivolutsky, D.A. 1983. *Radioecology of terrestrial animal communities*. Moscow: Energoatomizdat; 1983 (in Russian).
- Krivolutsky, D.A. 1987. Radiation ecology of soil animals. *Biol Fertil Soils*, 3: 51-55.
- Krivolutsky, D.A. 2000. Problems of Sustainable Development and Ecological Indication in Radioactively Contaminated Areas. *Russian Journal of Ecology*, 31 (4): 233-237.
- Krivolutsky, D.A., Pokarzhevsky, A.D. & Usachev, V.L. 1990. Effects of radioactive contamination of the environment on soil fauna in the Chernobyl NPP vicinity. *Ecology*, 6: 32–42 (in Russian).
- Krivolutzkii, D.A., Martushov, V. & Ryabtsev, I. 1999. Influence of radioactive contamination on fauna in the area of the Chernobyl NPP during first years after the accident (1986-1988). In: *Bioindicators of Radioactive Contamination*, Nauka, Moscow, pp. 106-122 (in Russian).
- Krivolutzkii, D.A. & Pokarzhevskii, A.D. 1992. Effects of radioactive fallout on soil animal populations in the 30 km zone of the Chernobyl atomic power station. *Science of The Total Environment*, 112, 1: 69-77.
- Krivolutzkii, D.A., Pokarzhevskii & A.D., Viktorov, A.G. 1992. Earthworm populations in soils contaminated by the chernobyl atomic power station accident, 1986-1988. *Soil Biology and Biochemistry*, 24 (12): 1729-1731.
- Lapied, E., Nahmani, J. & Rousseau G. 2009. Influence of texture and amendments on soil properties and earthworm communities. *Applied Soil Ecology*, 43, 241–249.
- Lapied, E., Moudilou, E., Exbrayat, J.-M., Oughton, D.E. & Joner, J.E. 2010. Silver nanoparticle exposure cause apoptotic response in the earthworm *Lumbricus terrestris* (Oligochaeta). *Nanomedicine* 5, 975-984.

- Lapied, E., Nahmani, J.Y., Moudilou, E., Chaurand, P., Labille, J., Rose, J., Exbrayat, J.M., Oughton, D.H. & Joner, E.J. 2011. Ecotoxicological effects of an aged TiO₂ nanocomposite measured as apoptosis in the anecic earthworm *Lumbricus terrestris* after exposure through water, food and soil. *Environment International*, 37 (6): 1105-1110.
- Lapied, E. 2014. DriloBASE - World Earthworm Database. DriloBASE Project, Telematix. website: <http://earthworms.info/>.
- Lavelle, P. 1983. The structure of earthworm communities. In "Earthworm Ecology: from Darwin to Vermiculture", by Satchell, J.E. (ed.), Chapman and Hall, London, pp. 449-466.
- Lavelle, P. & Spain, A.V. 2001. *Soil Ecology*. Kluwer Academic Publishers, Dordrecht, The Netherlands. 654pp.
- Lewis, K. 2000. Programmed Death in Bacteria . *Microbiology and Molecular Biology Reviews*, 64 (3), 503–514.
- Marks, D.H., Stein, E.A. & Cooper, E.L. 1981. Acid phosphatase changes associated with response to foreign tissue in the earthworm *Lumbricus terrestris*. *Comp. Biochem. Physiol.*, 68A, 681–683.
- Matisoff, G., Ketterer, M.E., Rosén, K., Mietelski, J.W., Vitko, L.F., Persson, H. & Lokas, E. 2011. Downward migration of Chernobyl-derived radionuclides in soils in Poland and Sweden. *Applied Geochemistry*, 26 (1): 105-115.
- Milochau, A., Lassègues, M. & Valembois, P. 1997. Purification, characterization and activities of two hemolytic and antibacterial proteins from coelomic fluid of the annelid *Eisenia fetida andrei*. *Biochim. Biophys. Acta*, 1337, 123-132.
- Morgan, J.E. & Morgan, A.J. 1998. The distribution and intracellular compartmentation of metals in the endoecic earthworm *Aporrectodea caliginosa* sampled from an unpolluted and a metal-contaminated site. *Environmental pollution*, 99, 167-175.
- Morgan, J.E. & Morgan, A.J. 1999. The accumulation of metals (Cd, Cu, Pb, Zn and Ca) by two ecologically contrasting earthworm species (*Lumbricus rubellus* and *Aporrectodea caliginosa*): implications for ecotoxicological testing. *Applied Soil Ecology*, 13, 9-20.
- Müller-Lemans, H. & Van Dorp, F. 1996. Bioturbation as a mechanism for radionuclide transport in soil: relevance of earthworms. *J. Environ. Radioact.* 31, 7-20.
- Nahmani, J., Lavelle, P., Lapied, E. & van Oort, F. 2003. Effects of heavy metal soil pollution on earthworm communities in the north of France. *Pedobiologia*, 47, 664-669.
- Nakamori, T., Yoshida, S., Kubota, Y., Ban-Nai, T., Kaneko, N., Hasegawa, M. & Itoh, R. 2008. Effects of acute gamma irradiation on *Folsomia candida* (Collembola) in a standard test. *Ecotoxicology and Environmental Safety*, 71: 590-596.
- Ning, S.B., Guo, H.L., Wang, L. & Song, Y.C. 2002 Salt stress induces programmed cell death in prokaryotic organism *Anabaena*. *Journal of Applied Microbiology*, 93, 15–28.

- Norwegian Radiation Protection Authority 2013. Målerapport fra oppmåling av doseraten i strålefeltet fra kobolt-60. Tekdok, 1: 1-13.
- OECD 1984. Guidelines for testing of chemicals. No 207. Earthworm acute toxicity test. Adopted 4th April 1984.
- Ou, J., Pan, F., Geng, P., Wei, X, Xie, G., Deng, J., Pang, X. & Liang, H. 2012. Silencing Fibronectin Extra Domain A Enhances Radiosensitivity in Nasopharyngeal Carcinomas Involving an FAK/Akt/JNK Pathway. *International Journal of Radiation Oncology*Biology*Physics*, 82(4): 685-691.
- Oughton, D.H., Agnero, A., Avila, R., Brown, J.E., Copplestone, D. & Gilek, M. 2008. Addressing uncertainties in the ERICA Integrated Approach. *J. Environ. Radioact.*, 99: 1384–92.
- Oughton, D.H., Hertel-Aas, T., Pellicer, E., Mendoza, E. & Joner, E.J. 2008. Neutron activation of engineered nanoparticles as a tool for tracing their environmental fate and uptake in organisms. *Environmental Toxicology and Chemistry*, 27: 1883-1887.
- Peeters-Joris, C. 2000. The lysosomal of earthworm chloragocytes: biochemical and morphological characterisation. *Comp. Biochem. Physiol.*, 126A, 323–340.
- Pokarzhevskii, A.D., Uspenskaya, E.Yu. & Filimonova, Zh.V. 2003. Global Radioactive Contamination Background in Terrestrial Ecosystems 13 Years after the Chernobyl Accident. *Russian Journal of Ecology*, 34 (2): 73-79.
- Prentø, P. 1986. Cellular and intracellular localisation of catalase and acid phosphatase in the midgut of *Lumbricus terrestris* L.: a cell fractionation study. *Comp. Biochem. Physiol.*, 83B : 385–390.
- Reichle, D.E., Witherspoon, J.P., Mitchel, M.J. & Styron, C.E. 1972. Effects of beta-gamma radiation of earthworms under simulated-fall-out conditions. In *Survival of Food Crops, and Livestock in the Event of Nuclear War* (D. W. Benson and A. H. Sparrow, Eds.), pp. 527-534. CONF-700909, U.S. Atomic Energy Commission, Washington, DC.
- Richards, K.S. 1977. Structure and function of the oligochaete epidermis (Annelida). *Symposia of the Zoological Society of London*, 39, 171-193.
- Richards, K.S. & Ireland, M.P. 1978. Glycogen-lead relationship in the earthworm *Dendrobaena rubida* from a heavy metal site. *Histochemistry*, 56, 55-64.
- Roberts, R. 2000. *Apoptosis in Toxicology*. Taylor & Francis, London, New York, 239 pp.
- Roch, P., Valembois, P., Davant, N. & Lassègues, M. 1981. Protein analysis of earthworm coelomic fluid. II – Isolation and biochemical characterization of the *Eisenia fetida andrei* factor (EFAF). *Comp. Biochem. Physiol.*, 69, 829-836.
- Roots, B.I. 1960. Some observations on the chloragogenous tissue of earthworms. *Comparative Biochemistry and Physiology*, 1, 218-226.

- Salvesen, G.S. 2002. Caspases: opening the boxes and interpreting the arrows. *Cell Death Differ.*, 9(1): 3-5.
- Samuilov, V.D., Oleskin, A.V. & Lagunova, E.M. 2000. Programmed Cell Death. *Biochemistry*, 65, 8, 873-887.
- Santos Amaral, A.F. & dos Santos Rodrigues, A. 2005. Metal accumulation and apoptosis in the alimentary canal of *Lumbricus terrestris* as a metal biomarker. *BioMetals*, 18, 199–206.
- Saran, S. 2000. Programmed cell death. *Current Science*, 78, 5, 575-586.
- Sarapultsev, B.I. & Geras'kin, S.A. 1993. Genetic grounds of radioresistance and the evolution. *Energoatomizdat, Moscow*.
- Sokal, R.R. & Rohlf, F.J. 1981. *Biometry: the principles and practice of statistics in biological research*, second ed. W.H. Freeman, New York.
- Sokolov, V.E., Ryabov, I.N., Ryabtsev, I.A., Kulikov, A.O., Tichomirov, F.A. & Shcheglov, A.I. 1994. Effect of radioactive contamination on the flora and fauna in the vicinity of Chernobyl nuclear power plant. *Sov. Sci. Rev. F. Physiol. Gen. Biol. Rev.*, 8: 1-124.
- Stürzenbaum, S.R., Andre, J., Kille, P. & Morgan, A.J. 2009. Earthworm genomes, genes and proteins: the (re)discovery of Darwin's worms. *Proc. Biol. Sci.*, 7, 276 (1658): 789–797.
- Suzuki, J. & Egami, N. 1983. Mortality of the earthworms, *Eisenia foetida*, after gamma-irradiation at different stages of their life-history. *J. Radiat. Res.*, 24: 209–220.
- Suzuki, J. & Egami, N. 1984. Radiation-induced damage and recovery from it in germ cells in the earthworm, *Eisenia foetida*. *J. Faculty Sci. Univ. Tokyo, Sec. IV Zool.*, 15: 329-342.
- Tyler, A.N., Carter, S., Davidson, D.A., Long, D.J. & Tipping, R. 2001. The extent and significance of bioturbation on Cs-137 distributions in upland soils. *Catena*, 43: 81-99.
- United Nations Chernobyl Forum - Expert Group "Environment" 2005. *Environmental Consequences of the Chernobyl Accident and Their Remediation: Twenty Years of Experience*. EGE Report, 254 pp.
- United Nations Scientific Committee on the Effects of Atomic Radiation 2000. *Sources and Effects of Ionizing Radiation*. Scientific Annex J within 2000 UNSCEAR Report to the General Assembly, NY.
- United Nations Scientific Committee on the Effects of Atomic Radiation 2011. *Sources and Effects of Ionizing Radiation*. Volume II, Scientific Annexes C, D and E within 2008 UNSCEAR Report to the General Assembly, NY.
- Valembois, P., Roch, P., Lassègues M. & Davant N. 1982. Bacteriostatic activity of a chloragogen cell secretion. *Pedobiologia*, 24, 191-195.

- Valembois, P., Lassègues, M., Roch, P. & Vaillier, J. 1985. Scanning electron-microscopic study of the involvement of coelomic cells in earthworm antibacterial defense. *Cell and Tissue Research*, 240, 479–484.
- Vandenbygaart, A.J., Protz, R., Tomlin, A.D. & Miller, J.J. 1998. Cs-137 as an indicator of earthworm activity in soils. *Applied Soil Ecology*, 9: 167-173.
- Varute, A.T. & More, N.K. 1972. Are chloragosomes in earthworm chloragogen cells lysosomes? *Acta Histochem.*, 44, 144–151.
- Varute, A.T. & More, N.K. 1973. Lysosomal acid hydrolases in the chloragogen cells of earthworms. *Comp. Biochem. Physiol.*, 45A, 607–653.
- White, P.A. & Claxton, L.D. 2004. Mutagens in contaminated soil: a review. *Mutation Research*, 567: 227–345.
- Wilding, C.S., Trikić, M.Z., Hingston, J.L., Copplestone, D. & Tawn, E.J. 2006. Mitochondrial DNA mutation frequencies in experimentally irradiated compost worms, *Eisenia fetida*. *Mutation Research*, 603: 56–63.
- Zellweger, T., Kiyama, S., Chi, K., Miyake, H., Adomat, H., Skov, K. & Gleave, M.E. 2003. Overexpression of the cytoprotective protein clusterin decreases radiosensitivity in the human LNCaP prostate tumour model. *BJU International*, 92(4): 463-469.

	10°C						20°C								
	Control			10mGy/h			Control			0,14mGy/h			10mGy/h		
	Value	Standard deviation	Significance	Value	Standard deviation	Significance	Value	Standard deviation	Significance	Value	Standard deviation	Significance	Value	Standard deviation	Significance
TUNEL	3,42	2,1	A	9,24	3,3	B	3,64	2,9	A	3,3	2,5	A	13,58	3,1	B
APOSTAIN	3,48	1,8	A	11,34	3,7	B	3,58	2,5	A	3,48	2,3	A	12,26	4,4	B
CASPASE 3	2,26	0,8	A	6,02	1,2	B	2,36	0,3	A	2,68	0,4	A	7,36	1,7	B

Annex A: Average number of apoptotic cells per mm², standard deviation and relative significance according to staining method, temperature and irradiation level, all studied tissues combined. A difference is considered as significant with a *p* value ≤ 0,05 (read the significance horizontally).

	10°C						20°C								
	Control			10mGy/h			Control			0,14mGy/h			10mGy/h		
	Value	Standard deviation	Significance	Value	Standard deviation	Significance	Value	Standard deviation	Significance	Value	Standard deviation	Significance	Value	Standard deviation	Significance
TUNEL	3,42	2,1	A	9,24	3,3	AB	3,64	2,9	A	3,3	2,5	A	13,58	3,1	B
APOSTAIN	3,48	1,8	A	11,34	3,7	B	3,58	2,5	A	3,48	2,3	A	12,26	4,4	B
CASPASE 3	2,26	0,8	A	6,02	1,2	A	2,36	0,3	A	2,68	0,4	A	7,36	1,7	A

Annex B: Average number of apoptotic cells per mm², standard deviation and relative significance according to staining method, temperature and irradiation level, all studied tissues combined. A difference is considered as significant with a *p* value ≤ 0,05 (read the significance vertically).

Method	Treatment	Temperature	Cuticle			Circular musculature			Longitudinal musculature			Intestinal epithelium			Cloragogenous matrix		
			Value	Standard deviation	Significance	Value	Standard deviation	Significance	Value	Standard deviation	Significance	Value	Standard deviation	Significance	Value	Standard deviation	Significance
TUNEL	Control 10mGy/h	10	2,7	2,3	A	2,5	1,5	A	3,4	2,4	A	3,2	1,7	A	5,3	2,4	A
			6,1	1,5	A	6,2	1,3	A	6	1,7	A	12,6	7,5	B	15,3	4,5	B
	Control 0,14mGy/h 10mGy/h	20	2,7	1,9	A	2,3	1,9	A	2,4	2	A	4,8	4	A	6	4,5	A
			2,4	0,5	A	2,1	1,7	A	1,7	1,3	A	5,3	4,9	A	5	4,1	A
APOSTAIN	Control 10mGy/h	10	2,9	1,1	A	2,7	1,8	A	2,3	0,3	A	4,2	3,4	A	5,3	4,5	A
			6,3	1,4	A	6,2	1,2	A	6,5	2,5	A	16,9	9,2	B	20,8	4,4	B
	Control 0,14mGy/h 10mGy/h	20	3,2	1,8	A	2,3	1,5	A	2,4	1,6	A	4,5	3,7	A	5,5	4,1	A
			2	1,8	A	2,2	1,9	A	1,8	1,5	A	5,3	2,7	B	6,1	3,7	B
CASPASE 3	Control 10mGy/h	10	1,8	1,4	B	0,4	0,2	A	2,4	0,4	BC	3,4	0,9	C	3,3	0,9	C
			4,2	0,5	A	4,1	0,8	A	6,1	2,6	AB	8,3	1,3	B	7,4	1	B
	Control 0,14mGy/h 10mGy/h	20	2,2	0,4	B	1,1	0,1	A	1,9	0,4	B	3,4	0,4	C	3,2	0,4	C
			1,7	0,2	B	0,7	0,3	A	1,6	0,4	B	4,9	0,3	C	4,5	0,8	C
			5,3	1,5	A	6	1,3	A	4,9	0,9	A	11,7	1,5	B	8,9	3,1	B

Annex C: Average number of apoptotic cells per mm² in each studied tissue, standard deviation and relative significance according to staining method, temperature and irradiation level. A difference is considered as significant with a *p* value ≤ 0,05 (read the significance horizontally).

Method	Treatment	Temperature	Cuticle			Circular musculature			Longitudinal musculature			Intestinal epithelium			Cloragogenous matrix		
			Value	Standard deviation	Significance	Value	Standard deviation	Significance	Value	Standard deviation	Significance	Value	Standard deviation	Significance	Value	Standard deviation	Significance
TUNEL	Control 10mGy/h	10	2,7	2,3	A	2,5	1,5	A	3,4	2,4	A	3,2	1,7	A	5,3	2,4	A
			6,1	1,5	A	6,2	1,3	A	6	1,7	A	12,6	7,5	B	15,3	4,5	B
	Control 0,14mGy/h 10mGy/h	20	2,7	1,9	A	2,3	1,9	A	2,4	2	A	4,8	4	A	6	4,5	A
			2,4	0,5	A	2,1	1,7	A	1,7	1,3	A	5,3	4,9	A	5	4,1	A
APOSTAIN	Control 10mGy/h	10	2,9	1,1	A	2,7	1,8	A	2,3	0,3	A	4,2	1,1	A	5,3	4,5	A
			6,3	1,4	A	6,2	1,2	A	6,5	2,5	A	16,9	9,2	B	20,8	4,4	B
	Control 0,14mGy/h 10mGy/h	20	3,2	1,8	A	2,3	1,5	A	2,4	1,6	A	4,5	3,7	A	5,5	4,1	A
			2	1,8	A	2,2	1,9	A	1,8	1,5	A	5,3	2,7	A	6,1	3,7	A
CASPASE 3	Control 10mGy/h	10	1,8	1,4	A	0,4	0,2	A	2,4	0,4	A	3,4	0,9	A	3,3	0,9	A
			4,2	0,5	B	4,1	0,8	B	6,1	2,6	B	8,3	1,3	C	7,4	1	C
	Control 0,14mGy/h 10mGy/h	20	2,2	0,4	A	1,1	0,1	A	1,9	0,4	A	3,4	0,4	A	3,2	0,4	A
			1,7	0,2	A	0,7	0,3	A	1,6	0,4	A	4,9	0,3	B	4,5	0,8	B
			5,3	1,5	B	6	1,3	C	4,9	0,9	B	11,7	1,5	D	8,9	3,1	C

Annex D: Average number of apoptotic cells per mm² in each studied tissue, standard deviation and relative significance according to staining method, temperature and irradiation level. A difference is considered as significant with a *p* value ≤ 0,05 (read the significance vertically).



Norwegian University
of Life Sciences

Postboks 5003
NO-1432 Ås, Norway
+47 67 23 00 00
www.nmbu.no